Normal Forms, Bifurcations and Limit Dynamics in Adaptive Control Systems

G.R. Rokni Lamooki, S. Townley
School of Mathematical Sciences
University of Exeter
Exeter EX4 4QE, UK
(Reza)(Townley)@maths.exeter.ac.uk

H.M. Osinga
Department of Engineering Mathematics
University of Bristol
Bristol BS8 1TR, UK
H.M.Osinga@bristol.ac.uk

Abstract

Adaptive controllers are used in systems where one or more parameters are unknown. Such controllers are designed to stabilize the system using an estimate for the unknown parameters that is adapted automatically as part of the stabilization. One drawback in adaptive control design is the possibility that the closed-loop limit system is not stable. The worst situation is the existence of a destabilized limit system attracting a large open subset of initial conditions.

These situations lie behind *bad behaviour* of the closed-loop adaptive control system. The main issue in this paper is to identify and characterize the occurrence of such bad behaviour in the adaptive stabilization of first- and second-order systems with one unknown parameter. We develop normal forms for all possible cases and find the conditions that lead to bad behaviour. In this context we discuss a number of bifurcation-like phenomena.

1 Preliminaries and motivation

Adaptive control is an established approach to the control of (parametrically) uncertain systems. Loosely speaking, there are two approaches to adaptive control: in one approach the adaptive controller tries to 'learn' the unknown parameters, the learning is guaranteed under suitable assumptions and the adaptive controller converges to a non-adaptive *limit controller* which is then itself guaranteed to be stabilizing; see for example [10, 11]. In a second so-called direct approach there is no attempt to learn the unknown parameters but instead the aim is simply to stabilize the system's dynamics. Again under suitable assumptions the adaptive controller converges to a limiting closed-loop system. However, there is no guarantee that the limit controller is stabilizing. In fact, the possibility that such destabilizing limit controllers can be the limit for a large open set of initial conditions, i.e. the phenomenon is generic, is of great concern. Such situations give rise to undesirable closed-loop behaviour of the adaptive control system. In this paper we aim to understand and characterize the occurence of such undesirable behaviour. From the viewpoint of dynamical systems theory, we are classifying normal forms for two- and three-dimensional systems. However, there is an added complication because the adaptive part of the controller causes the generic case to have one zero eigenvalue and there are also further degeneracies. This leads us to consider a number of different concepts of bifurcations.

This paper focusses on the class of adaptive back-stepping control for systems in strict feedback form. Let us, therefore, begin by explaining these notions. As a simple example, we consider a chain of two integrators given by

$$\begin{cases} \dot{x} &= f_1(x,y), \\ \dot{y} &= f_2(x,y,u), \end{cases} \tag{1}$$

where $f_1(0,0) = 0$ and $f_2(0,0,0) = 0$. The goal is to find a control u as a function of x and y such that the origin becomes asymptotically stable. The idea of back-stepping is to stabilize this system using feedback via two steps: in the first step we consider the $x-$equation and assume that y is the control signal. Hence, we try to find a suitable feedback $y = \kappa(x)$, such that the equilibrium $x = 0$ of the equation $\dot{x} = f_1(x, \kappa(x))$ is stabilized. In the next step we try to find the actual controller $u(x,y)$ such that the origin of Eq. (1) is stabilized. The idea is to design a feedback $u(x,y)$ such that both $x(t) \to 0$ and a dummy variable $z(t) = y(t) - \kappa(x(t)) \to 0$ as $t \to \infty$. This guarantees that $y \to \kappa(x)$. If $\kappa(0) = 0$ and κ is continuous, then this automatically implies $(x,y) \to 0$ for $t \to \infty$, as required. The Back-Stepping Theorem [19] guarantees the existence of a controller u with the required properties, provided f_1, f_2 and κ are smooth and $\kappa(0) = 0$.

In general, one can consider more than one step in this back-stepping approach. The concept of back-stepping is especially useful for systems in strict

feedback form. Such systems are described by

$$\begin{cases} \dot{x}_1 &= x_2 &+ \varphi_1(x_1), \\ \dot{x}_2 &= x_3 &+ \varphi_2(x_1, x_2), \\ &\vdots & \\ \dot{x}_{n-1} &= x_n &+ \varphi_{n-1}(x_1, x_2, \ldots, x_{n-1}), \\ \dot{x}_n &= u &+ \varphi_n(x_1, x_2, \ldots, x_n), \end{cases}$$

with $x_i \in \mathbb{R}$ and $\varphi_i(0) = 0$ for all $1 \leq i \leq n$, and $u \in \mathbb{R}$.

In order to explain the term adaptive control we consider a system

$$\dot{x} = f(x, u, \theta^*), \tag{2}$$

were $x \in \mathbb{R}^n$ is the state, $u \in \mathbb{R}^m$ is the input and $\theta^* \in \mathbb{R}^p$ is a fixed unknown parameter. We assume, independently of θ^*, that $x = 0$ is an equilibrium of the unforced system, so that $f(0, 0, \theta) = 0$ for all θ. An adaptive controller that stabilizes Eq. (2) about the equilibrium $x = 0$ takes the form

$$u = g(x, \hat{\theta}), \tag{3}$$

where $g(0, \hat{\theta}) = 0$ for all $\hat{\theta}$, and where the parameter $\hat{\theta}$ is adapted according to

$$\dot{\hat{\theta}} = G(x, \hat{\theta}). \tag{4}$$

Adaptive stabilization requires that each solution of the adaptive closed-loop system given by Eqs. (2)-(4) satisfies $x(t) \to 0$ as $t \to \infty$. The general set-up of Eqs. (2)-(4) encompasses various specific adaptive controllers, including universal adaptive controllers [16, 20] and adaptive back-stepping controllers [14, 21].

To illustrate adaptive back-stepping control, consider a two-dimensional system similar to Eq. (1), but with an extra fixed unknown parameter, that is, the system

$$\begin{cases} \dot{x} &= f_1(x, y, \theta^*), \\ \dot{y} &= f_2(x, y, u). \end{cases}$$

Adaptive back-stepping means that one first finds a feedback $y = \kappa(x)$ and an intermediate parameter adaptation $\dot{\hat{\theta}} = G^*(x, \hat{\theta})$ so that, in the first step, the closed-loop system

$$\begin{cases} \dot{x} &= f_1(x, \kappa(x), \theta^*), \\ \dot{\hat{\theta}} &= G^*(x, \hat{\theta}) \end{cases}$$

is $x-$stabilized, that is, $x(t) \to 0$ as $t \to \infty$. In the next step, we need to specify the actual controller u and the actual parameter adaptation law so that $z(t) = y(t) - \kappa(x(t)) \to 0$ and $x(t) \to 0$ as $t \to \infty$. Again, this implies that also

$y(t) \to 0$, provided $\kappa(0) = 0$ and κ is continuous. Adaptive back-stepping can be used for uncertain systems in strict feedback form:

$$\left\{\begin{array}{lcll} \dot{x}_1 & = & x_2 & + \varphi_1(x_1)^T \theta^*, \\ & \vdots & & \\ \dot{x}_{n-1} & = & x_n & + \varphi_{n-1}(x_1, \ldots, x_{n-1})^T \theta^*, \\ \dot{x}_n & = & u & + \varphi_n(x)^T \theta^*, \end{array}\right. \tag{5}$$

where, $\theta^* \in \mathbb{R}^p$ is a vector of unknown constant parameters. The $\varphi_i : \mathbb{R}^i \to \mathbb{R}^p$ in Eq. (5) are known smooth functions satisfying $\varphi_i(0) = 0$ for each $i = 1, \ldots, n$; see also [2, 13, 14, 21] for details.

Example 1 *Consider the following nonlinear scalar system taken from [21]:*

$$\dot{x} = u + \theta^* (x - b\, x^2).$$

This system has the form of Eq. (5) with $n = 1$, $p = 1$ and $\varphi_n(x) = \varphi_1(x) = x - b\, x^2$. The aim is to find a controller $u = g(x, \hat{\theta})$, where $\hat{\theta}$ is the parameter estimation which should be updated by a suitable adaptation law $\dot{\hat{\theta}} = G(x, \hat{\theta})$. Let us denote the error between the estimation parameter $\hat{\theta}$ and the actual unknown parameter θ^* by $k = \theta^* - \hat{\theta}$. Consider $V(x, k) = \frac{1}{2}(x^2 + k^2)$ as the Lyapunov function. Then we have

$$\begin{array}{rcl} \dot{V} & = & x\, \dot{x} + k\, \dot{k} \\ & = & x\, (u + \theta^* (x - b\, x^2)) + k\, (\dot{\hat{\theta}}) \\ & = & x\, (u + \hat{\theta}\, (x - b\, x^2)) + k\, (x\, (x - b\, x^2) - \dot{\hat{\theta}}). \end{array}$$

By using

$$u = -x - \hat{\theta}\, (x - b\, x^2) \quad \text{and} \quad \dot{\hat{\theta}} = x\, (x - b\, x^2),$$

we obtain

$$\dot{V} = -x^2,$$

so that $x(t) \to 0$ as $t \to \infty$ for the adaptive closed-loop system in the (k, x)-plane

$$\left\{\begin{array}{rcl} \dot{k} & = & -x\, (x - b\, x^2), \\ \dot{x} & = & -x + k\, (x - b\, x^2). \end{array}\right. \tag{6}$$

The phase portrait of system (6) is illustrated in Figure 1. Arbitrary initial conditions converge to the k-axis, which consists entirely of equilibria. Equilibria to the right of $(1, 0)$ (bright green) have empty basin of attraction while the equilibria to the left of $(1, 0)$ (dark green) have a one-dimensional basin of attraction. The equilibrium $(1, 0)$ itself (black dot) is special: it attracts a whole wedge of initial conditions, namely the yellow region marked Σ in Fig. 1; see [21] for the proof. This property leads to bad behaviour as will be explained later.

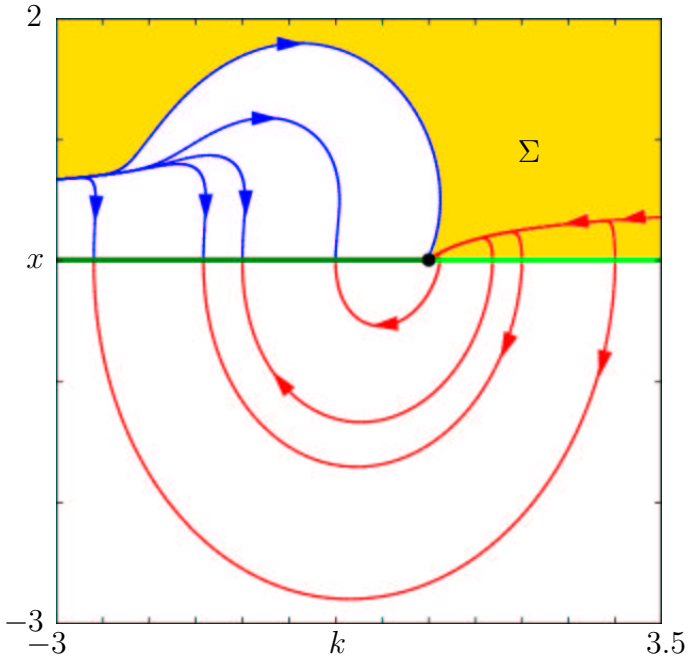

Figure 1: Phase portrait of the closed-loop system (6). The equilibrium $(k, x) = (1, 0)$ attracts a wedge-type set Σ of initial conditions while the limit system is not stabilized; see Example 1 for details. In this and all other figures the colour scheme is as follows: the equilibrium manifold is green, with stable equilibria dark green and unstable equilibria bright green. The critical point on the equilibrium manifold, which is a (potential) bad point, is marked by a black dot. Stable manifolds are coloured blue and unstable manifolds are red. Homoclinic or heteroclinic branches, which are (part of) both stable and unstable manifolds, are also coloured red.

Note that the adaptive closed-loop system given by Eqs. (2)-(4) is designed such that $x(t) \to 0$ as $t \to \infty$. However, the convergence of $\hat{\theta}(t)$ need not be achieved. Moreover, even if the parameter estimation converges, this need not mean that $\hat{\theta}(t)$ converges to the true value of the unknown parameter θ^*.

Let us assume that for any given initial value $(\hat{\theta}_0, x_0)$ in Eqs. (2)-(4) the parameter estimation $\hat{\theta}$ converges to a value $\hat{\theta}_\infty$ which will, in general, depend on the initial condition. Then, any initial condition $(\hat{\theta}_0, x_0)$ determines a fixed controller

$$u = g(x, \hat{\theta}_\infty). \tag{7}$$

This non-adaptive controller is a so-called *limit controller*; see [14, 16, 21]. Since $f(0, 0, \theta^*) = 0$ and $g(0, \hat{\theta}) = 0$, the origin $x = 0$ is an equilibrium for the corresponding *limit system* of the non-adaptive system (2) and (7), i.e.,

$$\dot{x} = f(x, g(x, \hat{\theta}_\infty), \theta^*). \tag{8}$$

The limit controller (7) (when it exists) is not guaranteed to yield a stabilized limit system (8). Surprisingly, failure of achieving a stabilized limit system can be quite dramatic, as is the case in Example 1. As mentioned above, the equilibrium $(k, x) = (1, 0)$ of Eq. (6) attracts a set of initial conditions with non-empty interior. However, the limit system

$$\dot{x} = -b\,x^2$$

corresponding to $k_\infty = 1$ has finite escape time and is thus unstable. Figure 1 shows that most initial conditions in the upper half of the (k, x)-plane converge to the limit system of $(k, x) = (1, 0)$. This means that we cannot confidently terminate the adaptation after some finite time and assume that the resulting frozen-time controller is stabilizing; see [14] for more details concerning this idea of frozen-time controller. Hence, in order for the adaptive controller to be stabilizing it must be *active* indefinitely. Note also that the basin of attraction of $(k, x) = (1, 0)$ forms a wedge with its tip at the equilibrium; see Figs. 1 and 4 (right). Therefore, orbits starting from nearby points can be pushed inside the basin by small disturbances.

In contrast, such dramatic failure does not seem to be possible in adaptive stabilization of linear systems. Linear systems are of the form

$$\begin{cases} \dot{x}(t) &= A\,x(t) + B\,u(t), \\ y(t) &= C\,x(t), \end{cases} \tag{9}$$

with $x \in \mathbb{R}^n$, $y \in \mathbb{R}^p$, $u \in \mathbb{R}^m$, and A and B matrices of appropriate sizes. The universal adaptive controller for this system is the control feedback law $u(t) = U(y(t), k(t))$ with a gain parameter $k(t)$ adapted according to the law $\dot{k} = K(y(t), k(t), u(t))$ such that for (unknown) matrices A and B and initial conditions $(k_0, x_0) \in \mathbb{R}^p \times \mathbb{R}^n$ the gain parameter $k(t)$ and the state $x(t)$ of the closed-loop system satisfy

$$x(t) \to 0 \quad \text{and} \quad k(t) \to k_\infty(k_0, x_0) \quad \text{as} \quad t \to \infty.$$

This problem has been studied in detail in [16] and [20]. The authors of [16] considered the class of single-input single-output minimum phase systems of (9) with adaptive feedback law $u(t) = -k(t)\,y(t)$ and the evolution law $\dot{k} = y(t)^2$. In [20] a more general class of multiple-input multiple-output systems with piecewise linear controllers has been considered. For the codimension-one case it is known that equilibria corresponding to unstable limit systems never attract an open set of initial conditions for these classes of universal adaptive controllers; see [17].

In universal adaptive control of scalar linear systems the organization of the behaviour yields, in a neighbourhood of the equilibrium manifold $x = 0$, local dynamics either corresponding to exponentially (un)stable limit systems or resembling either a *semi-centre* or a *semi-saddle*; see Fig. 2(a)-(b) and [20]. Similarly,

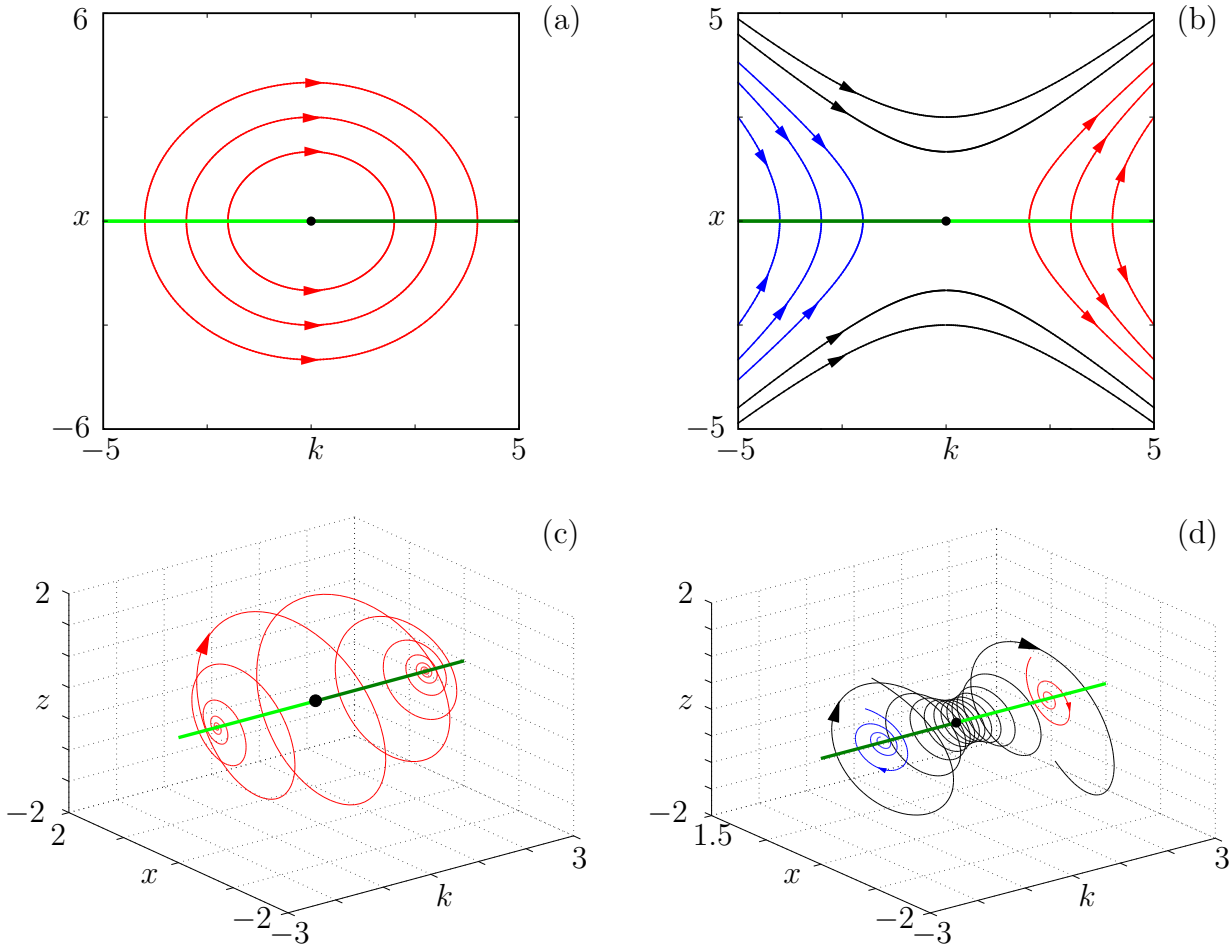

Figure 2: Possible local phase portrait for universal adaptive controllers of systems that are linear: for the scalar case we obtain a semi-centre (a) or a semi-saddle (b). For the two-dimensional case the controller leads to a spherical spiral (c) or a conical spiral (d); see Fig. 1 for an explanation of the colours.

the local behaviour for the universal adaptive control of two-dimensional linear systems is equivalent to the behaviour of non-critical limit systems or resembles either a *spherical-spiral* or a *conical-spiral*; see Fig. 2(c)-(d) and [16]. The non-linearity in Example 1 leads to new local behaviour resembling a single wedge.

We call system (8) a *bad limit system* if $x = 0$ is not a stable equilibrium. A bad limit system corresponding to a repelling equilibrium cannot cause any problems. However, as seen in Example 1, a bad limit system may occur at an equilibrium with a non-empty interior basin of attraction. Such an equilibrium is called a *bad equilibrium point* or abbreviated BP. We have seen single-wedge local behaviour in Example 1. This behaviour is, in some sense, a new bifurcation.

Appearance and disappearance of BPs is called a *bad equilibrium point bifurcation* or abbreviated BPB. The equilibrium $(k, x) = (1, 0)$ in Example 1 is both a BP and a BPB.

We investigate the occurrence of BPs and BPBs and, in particular, what kinds of degeneracy conditions lead to a BP or a BPB. To this end we focus on a specific class of systems to which we can apply adaptive back-stepping control. Namely, we consider nonlinear systems of the form

$$\dot{x} = f(x) + F(x)\,\theta^* + g(x)\,u, \quad x \in \mathbb{R}^n,\ u \in \mathbb{R},$$

that can be transformed into the strict feedback form of Eq. (5) using a parameter-independent smooth diffeomorphism [1, 11]. We also investigate the normal forms that arise around equilibria of the adaptive system (2)-(4) when Eq. (2) is in this strict feedback form. The adaptive closed-loop system for the n-dimensional equation (5) with a p-dimensional unknown parameter has state dimension $n+p$. We restrict our attention to the cases $1+1$ in Sec. 2 and $2+1$ in Sec. 3.

Our aims are three-fold: Firstly, we wish to identify all possible local behaviours, and thus qualitatively different organizations of closed-loop dynamics. We already determined the single-wedge, semi-centre and semi-saddle bifurcations for the closed-loop dynamics in the $1+1$ case and the spherical-spiral and conical-spiral bifurcations in the $2+1$ case; see also [16, 20]. Secondly, we want to make connections with recent developments of so-called *bifurcations without parameters*, again by locally classifying the possible closed-loop dynamics; see [5, 6, 7, 8]. Finally, we visualize the dynamics using DsTool [3] and a specially designed extension module [18].

Section 2 describes all possible local behaviour around the line of equilibria in the scalar case $1+1$. In this case, the only bifurcation without parameters is the transcritical bifurcation. In Sec. 3 we consider the case $2+1$, where a transcritical or a Hopf bifurcation can take place on the equilibrium manifold; see [15] for more details on these bifurcations in the general context of dynamical systems theory. In contrast to the $1+1$ case, the actual value of the unknown parameter θ^* plays a significant role in the $2+1$ case. In particular, more degenerate situations may occur. For example, θ^* may be such that a Bogdanov-Takens bifurcation occurs, i.e. a Hopf bifurcation where the pair of complex conjugate purely imaginary eigenvalues are actually both zero. The study of the $2+1$ case is not complete and we focus on the most likely possibilities of the dynamics. In particular, we only briefly discuss the Bogdanov-Takens bifurcation. In both cases $1+1$ and $2+1$ the adaptive closed-loop systems contain specific degeneracy conditions that are considered non-generic in standard dynamical systems theory. However, in the class of adaptive controllers such degeneracy conditions are generic, because of the form of the adaptation. This distinguishes our study from the existing dynamical systems' literature.

2 The $1+1$ case

In the scalar case, i.e., $n = p = 1$, system (5) becomes

$$\dot{x} = u + \theta^* \varphi(x), \qquad x,\, u,\, \theta^* \in \mathbb{R}. \tag{10}$$

As before, $\varphi(0) = 0$ so that $x = 0$ is an equilibrium of the uncontrolled system. Our goal is to stabilize $x = 0$, where we assume that the true value of the parameter θ^* is not known. Following the construction in Example 1, the adaptive (back-stepping) controller takes the form

$$u = -\mu(x) - \hat{\theta}\, \varphi(x), \tag{11}$$

where μ satisfies $x\, \mu(x) > 0$ for all $x \neq 0$, and $\mu(0) = 0$ (in Example 1 we used $\mu(x) = x$). The parameter estimate $\hat{\theta}$ is adapted according to

$$\dot{\hat{\theta}} = x\, \varphi(x). \tag{12}$$

If we again introduce the estimation error $k = \theta^* - \hat{\theta}$, then the closed-loop system (10)-(12) becomes:

$$\left\{ \begin{array}{rcl} \dot{k} & = & -x\, \varphi(x), \\ \dot{x} & = & -\mu(x) + k\, \varphi(x). \end{array} \right. \tag{13}$$

The k-axis is a line of equilibria and could contain bad equilibrium points. We are seeking a bifurcation diagram for BPs and BPBs on the equilibrium manifold $x = 0$. However, what do we mean by a bifurcation here? Each equilibrium on the line of equilibria has its own stability properties and associated limit system. The stability properties of either such an equilibrium or its associated limit system may change along the $k-$axis. As a consequence, we need to study the stability of all equilibria, their corresponding limit systems and their basins of attraction. The change of stability properties of the equilibria along the $k-$axis can be interpreted as a bifurcation. Such a bifurcation is referred to as a *bifurcation without parameters*, namely the bifurcation results from the dynamics of the system rather than the system parameters. The idea of bifurcations without parameters was introduced in [7] in the context of a generic Hopf bifurcation from lines of equilibria for two- and three-dimensional centre manifolds in order to study the loss of stability for hyperbolic and elliptic cases. This type of bifurcation is also addressed in [6] where a Bogdanov-Takens bifurcation without parameters was analysed. We use the same methodology for understanding the complex behaviour of adaptive control systems.

In this section, we determine all possible local behaviour of Eq. (13) in order to investigate the properties of the resulting limit system. Our aim is to see if there are other types of BPs in addition to the single wedge as seen in Example 1 of Sec. 1. We determine the normal form for a single-wedge bifurcation which is a BP, and the normal form for a *double-wedge* bifurcation which is not a BP.

2.1 Stability of the closed-loop system

Let us first investigate whether $x = 0$ is indeed stabilized. Note that the controller is constructed such that the Lyapunov function $V = \frac{1}{2}(x^2 + k^2)$ satisfies $\dot{V} = -x\,\mu(x) \leq 0$ for all x. In order to use LaSalle's Invariant Theorem [12] we consider (k, x) on the compact subset $\Omega_c = \{(k, x) \mid V \leq c^2\} \subset \mathbb{R}^2$ for some fixed $c > 0$. Our choice of μ guarantees that Ω_c is indeed a compact and positively invariant subset of $\mathbb{R}^2$ for Eq. (13). Let $E = \{(k, x) \in \Omega_c \mid \dot{V}(k, x) = 0\}$ and assume that M is the largest invariant subset of E. In fact, for Eq. (13) we have $M = E$ and since the $k-$axis is a line of equilibria, $M = \{(k, 0) \mid -c \leq k \leq c\}$. LaSalle's Theorem implies that all solutions starting from $(k_0, x_0) \in \Omega_c$ satisfy $(k(t), x(t)) \to M$ as $t \to \infty$. Therefore, we have $x(t) \to 0$ as $t \to \infty$. Note that $c > 0$ was chosen arbitrarily and for any initial condition $(k_0, x_0) \in \mathbb{R}^2$ there is $\bar{c} > 0$ such that $(k_0, x_0) \in \Omega_{\bar{c}}$. Hence, for all initial conditions $(k_0, x_0) \in \mathbb{R}^2$ we have that $x(t) \to 0$ as $t \to \infty$. In addition, for any initial condition $(k_0, x_0) \in \mathbb{R}^2$ there exists $k_\infty \in \mathbb{R}$ such that

$$\lim_{t\to\infty} x(t) = 0 \quad \text{and} \quad \lim_{t\to\infty} k(t) = k_\infty; \tag{14}$$

this is shown in [14]. Of course, k_∞ in Eq. (14) depends on k_0 and x_0. Given the adaptive system (13), any initial condition (k_0, x_0) determines a fixed limit controller

$$u = -\mu(x) - (\theta^* - k_\infty)\,\varphi(x). \tag{15}$$

Since both $\varphi(0) = 0$ and $\mu(0) = 0$, the point $x = 0$ is also an equilibrium of the corresponding limit system

$$\dot{x} = -\mu(x) + k_\infty\,\varphi(x).$$

We already pointed out in Sec. 1 that the limit controller (15) does not necessarily yield a stabilized limit system for all k_∞.

2.2 Normal form calculations

Consider system (13) with $\varphi(0) = 0$ and $\mu(0) = 0$. Since $x(t) \to 0$ as $t \to \infty$, let us assume that in a neighbourhood of $x = 0$ the functions φ and μ can be written as

$$\begin{aligned}
\varphi(x) &= \varphi_1\,x + \varphi_2\,x^2 + \cdots + \varphi_N\,x^N + O\left(x^{N+1}\right), \\
\mu(x) &= \mu_1\,x + \mu_2\,x^2 + \cdots + \mu_N\,x^N + O\left(x^{N+1}\right),
\end{aligned}$$

for N sufficiently large. Here, μ_i and φ_i are constants for all $1 \leq i \leq N$. Note that there are no constant terms in these polynomial expansions because of our assumption $\varphi(0) = \mu(0) = 0$. Furthermore, if u given by Eq. (11) is stabilizing,

then we must have $x\,\mu(x) > 0$ for all x. Hence, the first nonzero coefficient μ_i must have i odd and satisfy $\mu_i > 0$. The closed-loop system (13) becomes

$$\left\{ \begin{array}{rcl} \dot{k} &=& -\varphi_1\,x^2 \;-\; \varphi_2\,x^3 \;-\; \cdots, \\ \dot{x} &=& -\mu_1\,x \;-\; \mu_2\,x^2 \;-\; \cdots \;+\; k\,(\varphi_1\,x + \varphi_2\,x^2 + \cdots). \end{array} \right. \tag{16}$$

Normal form theory tells us that the local qualitative behaviour of the closed-loop system (13) near the $k-$axis is determined by the lower-order terms in the expansion of Eq. (16). In order to investigate which higher-order terms no longer influence the qualitative behaviour of the system, we start by studying the linearized vector field; for more details see [9, 15].

For now, we assume that $\mu_1 > 0$; the case $\mu_1 = 0$ is discussed in Sec. 2.4. The linear part of Eq. (16) at the equilibrium point $(k_\infty, 0)$ is:

$$\left[\begin{array}{cc} 0 & 0 \\ 0 & -\mu_1 + \varphi_1 k_\infty \end{array} \right]. \tag{17}$$

Since the entire $k-$axis consists of equilibria, one eigenvalue is always equal to zero. If for a particular point $(k_\infty, 0)$ the other eigenvalue is also zero, then we say that a bifurcation (without parameters) takes place on the k-axis at the point $(k_\infty, 0)$. Due to the presence of an invariant line, this bifurcation is a transcritical bifurcation. The matrix (17) indicates that such a transcritical bifurcation happens for $k_\infty = \mu_1/\varphi_1$, provided $\varphi_1 \neq 0$.

Let us first consider the case $\varphi_1 = 0$. Then (17) has one negative eigenvalue $-\mu_1$ and one zero eigenvalue. Since the entire $k-$axis consists of equilibria the centre manifold is trivial; as a result, all equilibria along the $k-$axis are locally attracting and all limit systems are locally stable. This case is illustrated in Fig. 3 for Eq. (13) with $\varphi(x) = 0.72\,x^2 + 0.25\,x^3$ and $\mu(x) = x$; see also [6].

2.3 Transcritical bifurcation without parameters

If $\varphi_1 \neq 0$ then the value of k_∞ does influence the dynamics and a transcritical bifurcation occurs along the k-axis. Let k_c denote the critical point $k_\infty = k_c = \frac{\mu_1}{\varphi_1}$ where $-\mu_1 + k_\infty\,\varphi_1 = 0$ in Eq. (17). As long as $k_\infty \neq k_c$, the matrix (17) has one nonzero eigenvalue $\varphi_1\,(k_\infty - k_c)$ and one zero eigenvalue. The centre manifold is again trivial so that the equilibrium $(k_\infty, 0)$ is attracting with a stable limit system if $\varphi_1\,(k_\infty - k_c) < 0$, and repelling if $\varphi_1\,(k_\infty - k_c) > 0$. Note that, even though the limit system in the latter case is unstable, such equilibria are not BPs, because their basins of attraction are empty.

At the critical point $k_c = \frac{\mu_1}{\varphi_1}$ the situation is different; the linearization fails and higher-order terms are needed. We introduce the change of variable $K := k - k_c = k - \frac{\mu_1}{\varphi_1}$ in Eq. (16) and rescale time as follows

$$t \mapsto \tau = \frac{1}{x}\,t, \tag{18}$$

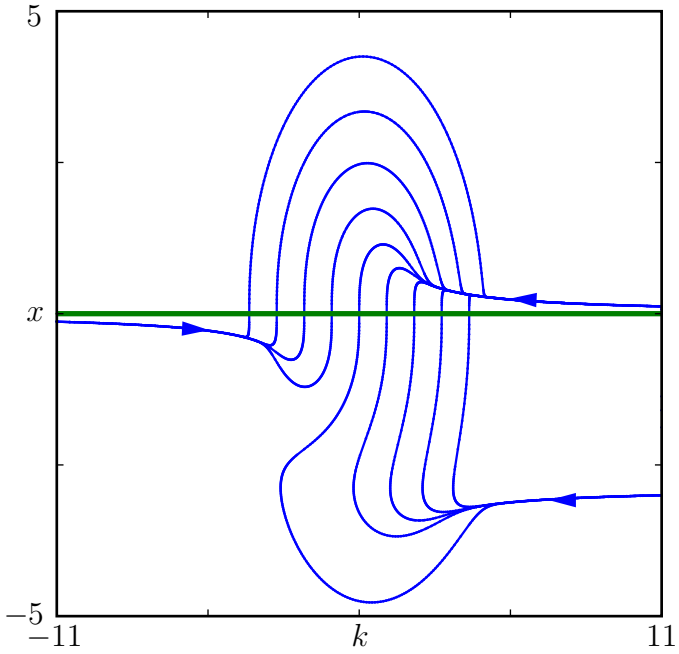

Figure 3: Phase portrait of Eq. (13) with $\varphi = 0.72\,x^2 + 0.25\,x^3$ and $\mu(x) = x$. The line of equilibria is globally attracting and all limit systems are stable. Consequently, there is no BP; see Fig. 1 for an explanation of the colours.

which in short notation is denoted by $'$. Note that this time-parametrization is singular at $x = 0$. The transformation (18) preserves the orbits in Eq. (16), but the *direction* of time is reversed in the lower half-plane $x < 0$; see also [4]. The resulting vector field is given by

$$\begin{cases} K' &= & - & \varphi_1\, x & + & O\,(x^2)\,, \\ x' &= \varphi_1\, K & + & \eta\, x & + & O(x)\, K + O\,(x^2)\,, \end{cases} \tag{19}$$

where $\eta = \mu_1 \frac{\varphi_2}{\varphi_1} - \mu_2$. The linearization at the origin of Eq. (19) is

$$\begin{bmatrix} 0 & -\varphi_1 \\ \varphi_1 & \eta \end{bmatrix} \tag{20}$$

with eigenvalues

$$s_{1,2} = \frac{1}{2}\left(\eta \pm \sqrt{\Delta}\right), \qquad \Delta = \eta^2 - 4\varphi_1^2.$$

Note that, due to the special form of the adaptive closed-loop system, the product of the eigenvalues is always positive. Hence, for the $1+1$ case the origin of the reduced system can never be a saddle. This property does not generalize to transcritical bifurcation points in higher-dimensional systems, as we shall see in Sec. 3.1 for the $2+1$ case.

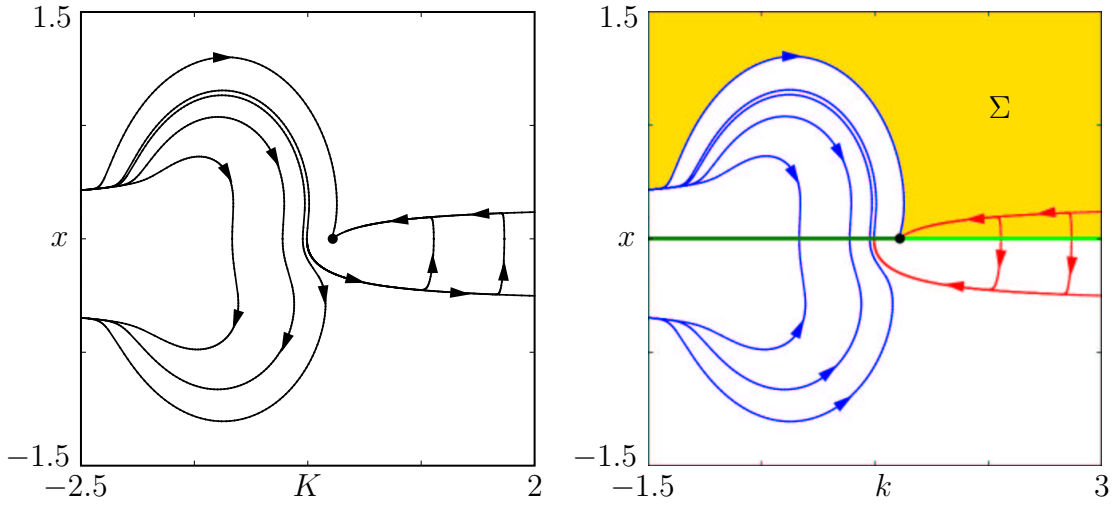

Figure 4: Visualization of the *single-wedge bifurcation* for $\varphi(x) = x - 2\,x^2 - 10\,x^3$ and $\mu(x) = x$ (so $\eta = -2$). The left panel shows the phase portrait of Eq. (16) after the transformation $K = k - 1$ and the time reparametrization (18). There is no line of equilibria and the origin is now a stable node. The right panel shows the phase portrait of the original system. It is obtained by reversing the direction of the flow in the lower half-plane of the phase portrait in the left panel. The k-axis is now a line of equilibria with a BP at $(1, 0)$ marked by a black dot. The region indicated by Σ is the basin of attraction of BP. The boundary of this set is formed by the half-line $\{(k, 0) \mid k \leq 1\}$ on the k-axis and the curve that is the limit of the strong stable manifolds of points $(1 - \varepsilon, 0)$ as $\varepsilon > 0$ goes to zero; see Fig. 1 for an explanation of the colours.

For $\Delta \geq 0$ and $\eta \neq 0$ both eigenvalues are real with the same sign as η. The direction of orbits for Eq. (16) are the same as for Eq. (19) if $x > 0$, but the direction is reversed if $x < 0$. Hence, the orbits of Eq. (16) stop or start at $x = 0$. Therefore, Eq. (16) has an attracting wedge at $(k_c, 0)$ in the lower half-plane if $\eta > 0$ or in the upper half-plane if $\eta < 0$. This is illustrated in Fig. 4 for $\varphi(x) = x - 2\,x^2 - 10\,x^3$ and $\mu(x) = x$.

The limit system at the critical point $k_\infty = k_c$,

$$\dot{x} = \eta\,x^2 + O\left(x^3\right),$$

is unstable with finite escape time, because $\eta \neq 0$. Hence, $(k_c, 0)$ is a bad equilibrium point, causing a bad point bifurcation. We call this critical point the *single-wedge bifurcation point* because it locally looks like a wedge; see Fig. 4. The bifurcation conditions for the single-wedge bifurcation point at $(k_c, 0) = (\frac{\mu_1}{\varphi_1}, 0)$

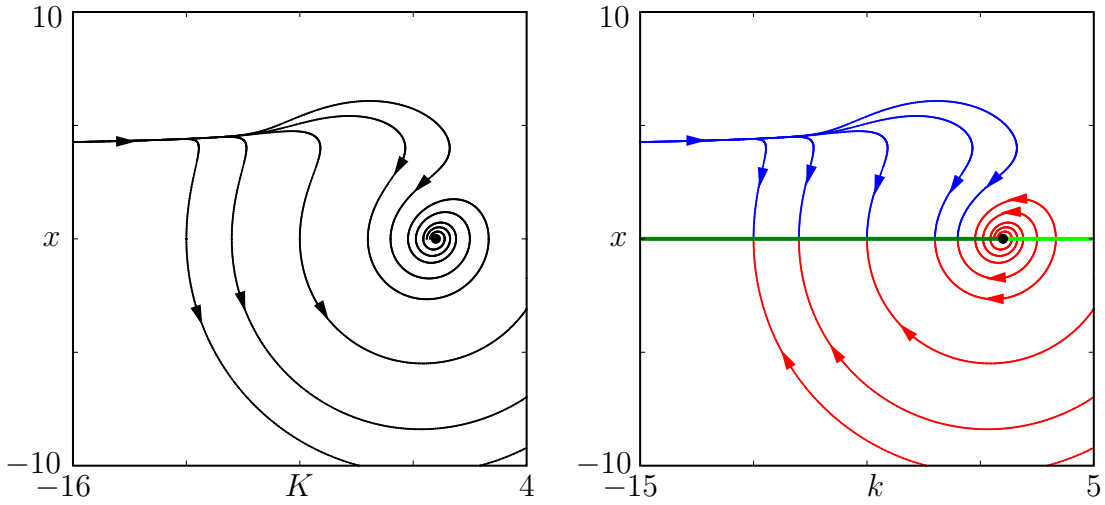

Figure 5: Visualization of the *semi-centre* for $\varphi(x) = x - 0.25\,x^2$ and $\mu(x) = x$ (so $\eta = -1$). The left panel shows the phase portrait of Eq. (16) after the transformation $K = k - 1$ and the time reparametrization (18). There is no line of equilibria and the origin is a stable spiral. The right panel shows the phase portrait of the original system, obtained by reversing the direction of the flow in the left picture for points in the lower half-plane. The resulting critical point is a semi-centre; see Fig. 1 for an explanation of the colours.

are:

$$\begin{cases} \mu_1 &= \dfrac{d}{dx}\,\mu(0) \neq 0, \\ \varphi_1 &= \dfrac{d}{dx}\,\varphi(0) \neq 0, \\ \eta &= \dfrac{1}{2}\left(\dfrac{\mu_1}{\varphi_1}\,\dfrac{d^2}{dx^2}\,\varphi(0) - \dfrac{d^2}{dx^2}\,\mu(0)\right) \neq 0, \\ \Delta &= \eta^2 - 4\,\varphi_1^2 \geq 0. \end{cases} \tag{21}$$

If $\Delta < 0$ and $\eta \neq 0$, then the eigenvalues of (20) are complex conjugate; see also Fig. 5 (left). This means that the critical point $(k_c, 0)$ is a semi-centre for Eq. (16). An example of this case is shown in Fig. 5 with $\varphi(x) = x - 0.25\,x^2$ and $\mu(x) = x$. The phase portrait in Fig. 5 (right) shows that the basin of attraction of the critical point is empty and there are no bad equilibrium points.

Finally, we consider the case $\eta = 0$. As before the linearization fails; the matrix (20) has a pair of purely imaginary eigenvalues and yields no information. Hence, we need to incorporate higher-order terms. We use the normal form of

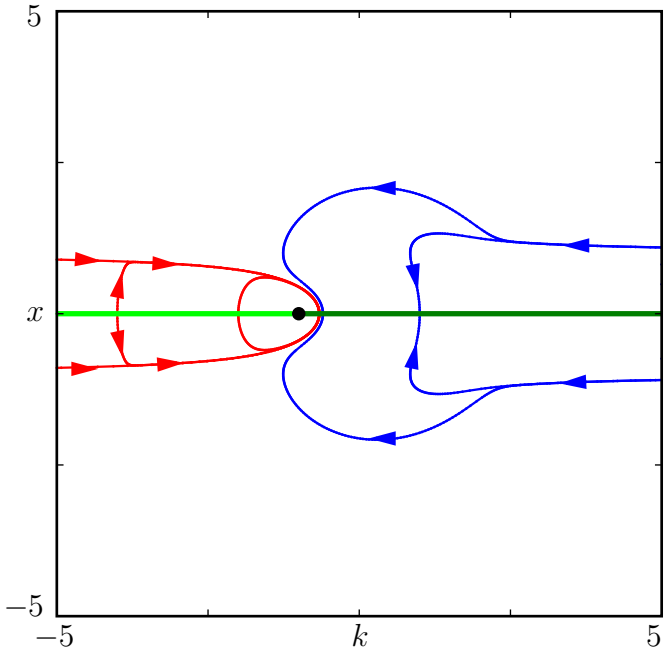

Figure 6: Phase portrait for the case $\eta = 0$ with $\varphi(x) = -x + x^3$ and $\mu(x) = x$. The critical point is a semi-centre; see Fig. 1 for an explanation of the colours.

Eq. (19) in polar coordinates as given in [9], namely

$$\begin{cases} \dot{r} &= a_1\, r^3 &+ a_2\, r^5 &+ \cdots, \\ \dot{\psi} &= \varphi_1 &+ b_1\, \psi^2 &+ \varphi_2\, \psi^4 &+ \cdots, \end{cases} \tag{22}$$

for certain constants a_i and b_i. The first nonzero coefficients in Eq. (22) determine the qualitative dynamics. There can be stable or unstable spiralling equilibria and periodic orbits. Since we used the time-reparametrization (18), this means that the equilibrium $(k_c, 0)$ in the original system (16) is always a centre. Hence, the basin of attraction of the critical point is again empty and there are no bad equilibrium points. An illustration of the case $\eta = 0$ is given in Fig. 6 for $\varphi(x) = -x + x^3$ and $\mu(x) = x$.

2.4 The double wedge

Recall that, so far, we assumed $\mu_1 \neq 0$. If $\mu_1 = 0$ then $\mu(x)$ has no linear term. However, then there can also be no quadratic term, because we require $x\,\mu(x) > 0$. Hence, let us assume that $\mu_3 \neq 0$. System (16) becomes

$$\begin{cases} \dot{k} &= -\varphi_1\, x^2 &- \varphi_2\, x^3 &- \cdots, \\ \dot{x} &= -\mu_3\, x^3 &- \cdots &+ k\,(\varphi_1\, x + \varphi_2\, x^2 + \cdots). \end{cases} \tag{23}$$

The critical point is now always at the origin $k_c = 0$. Proceeding as before, we find that for $\varphi_1 \neq 0$ Eq. (23) has a phase portrait that is topologically equivalent to that in Fig. 6. On the other hand, if $\varphi_1 = 0$, we need to incorporate higher-order terms. The time-reparametrization is now

$$t \mapsto \tau = \frac{1}{x^2}\, t, \tag{24}$$

which we again denote by $'$ for convenience. The resulting system is

$$\left\{ \begin{array}{rclcrcrcl} k' & = & -\varphi_2\, x & - & \varphi_3\, x^2 & - & \cdots, & & \\ x' & = & -\mu_3\, x & - & \mu_4\, x^2 & - & \cdots & + & k\,(\varphi_2 + \varphi_3\, x + \cdots). \end{array} \right. \tag{25}$$

Note that such a time reparametrization does not change the direction of the flow. The linearization of Eq. (25) at the origin is given by the matrix

$$\left[\begin{array}{cc} 0 & -\varphi_2 \\ \varphi_2 & -\mu_3 \end{array} \right].$$

We first assume that $\varphi_2 = 0$. Then the linearization is not hyperbolic. By relabelling the parameters to

$$\tilde{h}_i = \mu_{i+2}, \quad \tilde{\varphi}_i = \varphi_{i+2} \quad \text{for all} \quad i = 1, 2, 3, \ldots,$$

we obtain the system

$$\left\{ \begin{array}{rclcrcrcl} k' & = & -\tilde{\varphi}_1\, x^2 & - & \tilde{\varphi}_2\, x^3 & - & \cdots, & & \\ x' & = & -\tilde{h}_1\, x & - & \tilde{h}_2\, x^2 & - & \cdots & + & k\,(\tilde{\varphi}_1\, x + \tilde{\varphi}_2\, x^2 + \cdots), \end{array} \right.$$

which has the same form as Eq. (16). Hence, the original system (23) is a time reparametrization of Eq. (16) and does not yield a new case.

On the other hand, if $\varphi_2 \neq 0$, then the eigenvalues of Eq. (25) are hyperbolic

$$s_{1,2} = \frac{1}{2}\left(-\mu_3 \pm \sqrt{\mu_3^2 - 4\,\varphi_2^2} \right).$$

The situation is now very similar to the cases shown in Figs. 4 and 5, but the time reparametrization does not induce a reversal of the flow. If $\mu_3^2 - 4\varphi_2^2 < 0$ then the origin of system (25) is a stable focus. Hence, locally near $(k_c, 0)$ in the original system (23), each equilibrium has heteroclinic connections to two other equilibria, except for the semi-centre $(k_c, 0)$ itself. If $\mu_3^2 - 4\varphi_2^2 \geq 0$ then the origin of system (25) is a stable node. Locally near $(k_c, 0)$, each equilibrium in Eq. (23) has now one heteroclinic connection to $(k_c, 0)$. Therefore, the basin of attraction of $(k_c, 0)$ consists of a *double wedge*. The critical point $(k_c, 0) = (0, 0)$ is not a bad equilibrium point, because the corresponding limit system

$$\dot{x} = -\mu_3\, x^3 + \cdots$$

is asymptotically stable. A phase portrait for this case is shown in Fig. 7 with $\varphi(x) = 0.25\, x^2$ and $\mu(x) = x^3$.

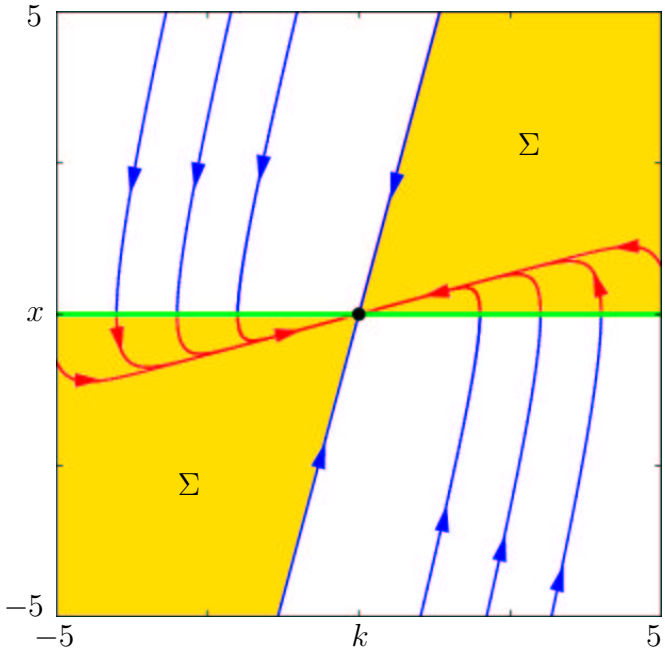

Figure 7: Visualization of an attracting *double-wedge* critical point for $\varphi(x) = 0.25\,x^2$ and $\mu(x) = x^3$. Here, the origin attracts a non-empty interior set Σ of initial conditions, but the corresponding limit system is attracting. The boundary of Σ is formed by the k-axis and the limits for $\varepsilon \to 0$ of the strong stable manifolds of equilibria $(\pm\varepsilon, 0)$; see Fig. 1 for an explanation of the colours.

2.5 Discussion

In this section we studied the scalar case of adaptive back-stepping control. We have investigated the stability types of equilibria of the closed-loop system (13) by assuming that we could rewrite it as Eq. (16). The analysis in the previous section reveals that the dynamics is organized by the first nonzero coefficients of the expansion of μ about $x = 0$.

If $\mu_1 \neq 0$ then we may encounter the *single-wedge bifurcation*, which is characterized by the bifurcation conditions (21); see Fig. 4 for the typical phase portrait. This bifurcation is a so-called bifurcation without parameters, due to the existence of a line of equilibria. The bifurcation conditions (21) suggest that the occurrence of the single-wedge bifurcation is of co-dimension one.

For the $1+1$ case there is a total of six topologically different phase portraits. Namely, if the system is linear the dynamics looks like a semi-centre as in Fig. 2 (a) or a semi-saddle as in Fig. 2 (b). For nonlinear systems with the adaptive back-stepping controller designed such that $\mu_1 \neq 0$ the dynamics could lead to globally attracting behaviour as in Fig. 3, where $\varphi_1 = 0$; if Eqs. (21) are satisfied, then one obtains the single-wedge bifurcation as illustrated in Fig. 4; Finally, one

may obtain the nonlinear version of the semi-centre, as in Fig. 5, or the centre illustrated in Fig. 6. If the adaptive back-stepping controller is designed using $\mu_1 = 0$, and thus $\mu_2 = 0$ as well, but $\mu_3 \neq 0$, then one obtains the double-wedge dynamics; see Fig. 7. In contrast to the single wedge, this is not a BPB.

Of course, more coefficients of the expansion for μ could be zero. However, we can always transform the system using flow-reversing or flow-preserving time reparametrizations similar to (18) or (24) and obtain phase portraits of the above six types. Hence, from the design point of view, unless $\frac{d}{dx}\,\varphi(0) = 0$ in Eq. (16), one must carefully choose the adaptive controller such that bad behaviour, that is, the single-wedge bifurcation, is avoided. This can be done, for example, by choosing μ_1 and μ_2 such that $\eta = \mu_1 \frac{\varphi_2}{\varphi_1} - \mu_2 = 0$. Clearly, such a controller depends sensitively on the (known) system parameters, i.e. on $\varphi(x)$, and is thus not robust.

It is possible to design an adaptive back-stepping controller that is more robust and avoids bad behaviour. Namely, let us introduce an extra parameter ϱ in the Lyapunov function used to derive the controller:

$$V(x,k) = \frac{1}{2}\left(x^2 + \frac{k^2}{\varrho}\right).$$

The estimate $\hat{\theta}$ should then be adapted according to

$$\dot{\hat{\theta}} = \varrho\, x\, \varphi(x)$$

and the closed-loop system becomes

$$\left\{ \begin{array}{rcl} \dot{k} &=& \varrho\ (\ -\varphi_1\, x^2 \ -\ \varphi_2\, x^3 \ -\ \cdots\ )\ , \\ \dot{x} &=& \quad -\mu_1\, x \ -\ \mu_2\, x^2 \ -\ \cdots + k\,(\varphi_1\, x + \varphi_2\, x^2 + \cdots). \end{array} \right.$$

Again, a transcritical bifurcation occurs for $(k_c, 0) = (\frac{\mu_1}{\varphi_1}, 0)$, but the linearization of the reduced system at the critical point is now given by

$$\left[\begin{array}{cc} 0 & -\varrho\,\varphi_1 \\ \varphi_1 & \eta \end{array} \right],$$

where $\eta = \mu_1 \frac{\varphi_2}{\varphi_1} - \mu_2$ as before; compare with Eq. (20). Hence, in order to avoid the single-wedge bifurcation, one needs to adjust ϱ such that

$$\Delta = \eta^2 - 4\varrho\,\varphi_1^2 < 0 \quad \Leftrightarrow \quad \varrho > \frac{\eta^2}{4\varphi_1^2}.$$

Note that in the $1+1$ case the actual value of the unknown parameter θ^* does not have any effect on the pattern of bifurcation without parameters. It simply results in a shift of the global dynamics along the line of equilibria. This is not necessarily the case in higher dimensions, as is shown in the next section for the $2+1$ case.

3 The $2+1$ case

In two dimensions the strict feedback form becomes

$$\begin{cases} \dot{x} &= y + \theta^* \varphi(x), \\ \dot{y} &= u, \end{cases} \tag{26}$$

where $x, y \in \mathbb{R}$ form the state, $u \in \mathbb{R}$ is the control and $\theta^* \in \mathbb{R}$ is the unknown parameter.

Similar to the approach in Example 1, we can stabilize the origin $(x, y) = (0, 0)$ using an adaptive back-stepping controller. This stabilization is done in two steps: first, we stabilize x by assuming that y is a control, which leads to the requirement $y = -\mu(x) - \hat{\theta}\,\varphi(x)$ with $\hat{\theta}$ the estimate for θ^*. Next, we stabilize both x and $z = y + \mu(x) + \hat{\theta}\,\varphi(x)$ using an appropriate controller $u = u(x, y)$. The construction, which is explained in detail in Appendix A, leads to the closed-loop system

$$\begin{cases} \dot{k} &= -\varphi(x)\,\left[x + z\,\left(\frac{d}{dx}\mu(x) + \frac{d}{dx}\varphi(x)\,[\theta^* - k]\right)\right], \\ \dot{x} &= -\mu(x) + z + k\,\varphi(x), \\ \dot{z} &= -x - \nu(z) + \left(\frac{d}{dx}\mu(x) + \frac{d}{dx}\varphi(x)\,[\theta^* - k]\right)\,k\,\varphi(x), \end{cases} \tag{27}$$

where $z = y + \mu(x) + \hat{\theta}\,\varphi(x)$ and $k = \theta^* - \hat{\theta}$ as before.

The adaptive stabilization yields $(x, z) \to (0, 0)$ and $k \to k_\infty$, the value of which depends on the initial conditions. Hence, $(x, z) = (0, 0)$ is a globally attracting equilibrium manifold of Eq. (27). In order to investigate the possible dynamics near this equilibrium manifold, we assume that φ, μ and ν can be written as

$$\begin{aligned} \varphi(x) &= \varphi_1\,x + \varphi_2\,x^2 + \cdots + \varphi_N\,x^N + O\left(x^{N+1}\right), \\ \mu(x) &= \mu_1\,x + \mu_2\,x^2 + \cdots + \mu_N\,x^N + O\left(x^{N+1}\right), \\ \nu(z) &= \nu_1\,z + \nu_2\,z^2 + \cdots + \nu_N\,z^N + O\left(z^{N+1}\right), \end{aligned}$$

for sufficiently large N. Similar to Sec. 2 the assumptions for both μ and ν imply that their first nonzero coefficients are positive and correspond to an odd power.

As in the previous section, we begin our investigation by considering the linearization of Eq. (27) at the equilibrium $(k_\infty, 0, 0)$. Note that $\frac{d}{dx}\varphi(0) = \varphi_1$, $\frac{d}{dx}\mu(0) = \mu_1$ and $\frac{d}{dx}\nu(0) = \nu_1$, so that the linearization becomes

$$\begin{bmatrix} 0 & 0 \\ 0 & A \end{bmatrix} = \left[\begin{array}{c|cc} 0 & 0 & 0 \\ \hline 0 & -\mu_1 + \varphi_1\,k_\infty & 1 \\ 0 & -1 + (\mu_1 + \varphi_1\,(\theta^* - k_\infty))\,\varphi_1\,k_\infty & -\nu_1 \end{array}\right]. \tag{28}$$

In contrast to the $1+1$ case, this linearization depends independently on both k_∞ and the actual value of the unknown parameter θ^*; compare Eq. (17). This

means, in particular, that the stability type of a given equilibrium of the closed-loop system and the behaviour of the corresponding limit system can depend on θ^*. This observation leads us to yet another notion of bifurcation in the context of adaptive control, namely, so-called *bifurcation with respect to unknown parameters*. Such a bifurcation cannot happen in the $1+1$ case.

The k-axis is again a line of equilibria so that the linearization (28) always has one eigenvalue equal to zero. A bifurcation (without parameters) takes place on the k-axis at the point $(k_\infty, 0, 0)$ for which additional eigenvalues are on the imaginary axis. If only one additional eigenvalue is zero, this corresponds to a transcritical bifurcation similar to the $1+1$ case; this bifurcation is discussed in Sec. 3.1 below. When the two additional eigenvalues form a purely imaginary complex conjugate pair, a Hopf bifurcation takes place; see Sec. 3.2. Finally, all three eigenvalues could be zero, which corresponds to a Bogdanov-Takens bifurcation; this bifurcation is of codimension two and we only encounter it for a particular value of the unknown parameter θ^*. The Bogdanov-Takens bifurcation would occur generically in the case $2+2$, which is discussed in detail in [6]. In the context of adaptive back-stepping control for the case $2+1$ we briefly discuss the Bogdanov-Takens bifurcation in Sec. 3.3, where we describe the dependency of these bifurcations on the unknown parameter θ^*.

3.1 Transcritical bifurcation in the $2+1$ case

A transcritical bifurcation takes place if there are exactly two eigenvalues equal to zero. This means that the matrix A in (28) must have one zero and one nonzero eigenvalue, that is, $\det A = 0$ and $\operatorname{trace} A \neq 0$. Note that the system is not stabilized unless the third eigenvalue is stable. Hence $\operatorname{trace} A < 0$ and we obtain the conditions

$$\begin{aligned} \varphi_1^2\, k_\infty^2 - (\mu_1 + \nu_1 + \theta^*\,\varphi_1)\;\varphi_1\, k_\infty + \mu_1\,\nu_1 + 1 &= 0, && (29)\\ \varphi_1\, k_\infty - \mu_1 - \nu_1 &< 0. && (30) \end{aligned}$$

Since both $\nu_1 \geq 0$ and $\mu_1 \geq 0$, we observe that Eq. (29) can only be satisfied if $\varphi_1 \neq 0$. Hence, similar to the $1+1$ case, there is no transcritical bifurcation if $\varphi_1 = 0$.

The possible local phase portraits for the transcritical bifurcation are now similar to the $1+1$ case, since this bifurcation takes place on a $(1+1)$-dimensional centre manifold. The centre manifold reduction is straightforward and discussed in detail in Appendix B. The resulting system is of the form

$$\left\{ \begin{array}{rcl} \dot K &=& \hat a\, v^2 \;+\; v\, g_1(K,v), \\ \dot v &=& \hat b\, K\, v \;+\; \hat c\, v^2 \;+\; v\, g_2(K,v). \end{array} \right. \qquad (31)$$

Here $K = k - k_c$ is used to shift the transcritical bifurcation at $k = k_c$ to the origin. The v-axis is the eigenspace corresponding to the zero eigenvalue of the

submatrix A in the linearization (28). The functions g_1 and g_2 are of order higher than two. We derive in Appendix B that the coefficients are

$$\begin{cases} \hat{a} &= -\varphi_1 \left[(\mu_1 - \nu_1)(\mu_1 - \varphi_1 k_c) + \varphi_1 \mu_1 \theta^* \right], \\ \hat{b} &= -\dfrac{\varphi_1}{\lambda_3} \left[\mu_1 + \nu_1 + \theta^* \varphi_1 - 2\varphi_1 k_c \right] = \varphi_1 - \dfrac{\varphi_1^2}{\lambda_3}(\theta^* - k_c), \\ \hat{c} &= -\dfrac{1}{\lambda_3} \left[\varphi_2 k_c \left(\mu_1 + \nu_1 + 3\varphi_1 [\theta^* - k_c] \right) \right. \\ & \qquad \left. -\nu_1 \mu_2 + 2\varphi_1 \mu_2 k_c - \nu_2 (\mu_1 - \varphi_1 k_c)^2 \right], \end{cases} \tag{32}$$

where $\lambda_3 = \varphi_1 k_c - \mu_1 - \nu_1 < 0$ is the third eigenvalue of the Jacobian at the critical point.

The dynamics close to the transcritical bifurcation point $(k_c, 0, 0)$ on the equilibrium manifold is determined by the dynamics on the centre manifold as given by Eq. (31). A time-reparametrization as defined in Eq. (18) leads to division by v in this system, so that we obtain equations of the same form as system (19). Hence, the linearization becomes

$$\begin{bmatrix} 0 & \hat{a} \\ \hat{b} & \hat{c} \end{bmatrix}.$$

Recall from Sec. 2.3 that the product of the eigenvalues for the $1+1$ case is $\varphi_1^2 > 0$. Hence, the eigenvalues are always both stable or both unstable. This property is special to the $1+1$ case. For higher-dimensional systems, one can have a saddle-type transcritical bifurcation on the centre manifold; for the $2+1$ case this happens when $\hat{a}\,\hat{b} > 0$. Locally in a neighbourhood of a saddle-type transcritical bifurcation point the equilibrium manifold is attracting only on one side of the critical point and most initial conditions leave this neighbourhood. Since the adaptive controller is designed so that eventually all initial conditions converge to the equilibrium manifold, another critical point must exist on the k-axis. Indeed, the transcritical bifurcation points come in pairs, defined by Eq. (29), and only one of these can be of saddle-type.

If $\hat{a}\,\hat{b} < 0$, we may encounter the three-dimensional version of the single-wedge bifurcation discussed in Sec. 2.3. Namely, for k_c such that (29) and (30) are satisfied, that is,

$$\begin{aligned} \varphi_1^2 k_c^2 - (\mu_1 + \nu_1 + \theta^* \varphi_1)\, \varphi_1 k_c + \mu_1 \nu_1 + 1 &= 0, \\ \varphi_1 k_c - \mu_1 - \nu_1 &< 0, \end{aligned}$$

a single-wedge bifurcation occurs at $(k_c, 0, 0) \in \mathbb{R}^3$, if the following conditions are satisfied:

$$\begin{cases} \hat{a}\,\hat{b} &< 0, \\ \hat{c}^2 + 4\,\hat{a}\,\hat{b} &\geq 0, \end{cases} \tag{33}$$

where $\hat{a}$, $\hat{b}$ and $\hat{c}$ are defined in Eq. (32). These bifurcation conditions are similar to those for the $1+1$ case given by (21). The phase portraits are also similar, except for an additional stable direction along the k-axis. In particular, locally near a single-wedge bifurcation the phase portrait shows an open basin of attraction for the critical point $(k_c, 0, 0)$ formed by an invariant cone. As in the $1+1$ case, the limit system is unstable at this critical point provided $\hat{c} \neq 0$. Note that this is automatically satisfied when $\hat{c}^2 + 4\,\hat{a}\,\hat{b} \geq 0$ and $\hat{a}\,\hat{b} < 0$. The unknown parameter θ^* plays an important role in the $2+1$ case. Not only does the location of the critical point $(k_c, 0, 0)$ depend on θ^*, but θ^* also determines whether this point is a BP or not, because $\hat{a}$, $\hat{b}$ and $\hat{c}$ depend on θ^* as well.

As an example of the single-wedge bifurcation in the $2+1$ case we consider

$$\varphi(x) = x, \quad \mu(x) = 2\,x \quad \text{and} \quad \nu(z) = 2\,z + 18\,z^2 + 41\,z^3,$$

so that the closed-loop system is given by

$$\left\{ \begin{array}{rcl} \dot{k} &=& -x^2 - (2+\theta^*)\,x\,z + k\,x\,z, \\ \dot{x} &=& -2\,x + z + k\,x, \\ \dot{z} &=& -x - 2\,z - 18\,z^2 - 41\,z^3 + (2+\theta^*)\,k\,x - k^2\,x. \end{array} \right. \tag{34}$$

Potential single-wedge bifurcation points are critical points $(k_c, 0, 0)$ with

$$k_c^2 - (4+\theta^*)\,k_c + 5 = 0 \Leftrightarrow k_c = \frac{4+\theta^*}{2} \pm \frac{1}{2}\sqrt{(4+\theta^*)^2 - 20}$$

and

$$\lambda_3 := k_c - 4 < 0.$$

Then Eq. (32) gives

$$\left\{ \begin{array}{rcl} \hat{a} &=& -2\,\theta^*, \\ \hat{b} &=& \dfrac{-1}{k_c - 4}\,(4 + \theta^* - 2\,k_c), \\ \hat{c} &=& \dfrac{18}{k_c - 4}\,(2 - k_c)^2. \end{array} \right.$$

The choice for θ^* must be such that Eqs. (33) are satisfied, that is,

$$\left\{ \begin{array}{rcll} \hat{a}\,\hat{b} &=& \dfrac{2\,\theta^*}{k_c - 4}\,(4 + \theta^* - 2\,k_c) & < \ 0, \\ \hat{c}^2 + 4\,\hat{a}\,\hat{b} &=& \dfrac{18^2}{(k_c-4)^2}\,(2-k_c)^4 + \dfrac{8\,\theta^*}{k_c - 4}\,(4 + \theta^* - 2\,k_c) & \geq \ 0. \end{array} \right.$$

We take $\theta^* = 2$ so that the critical point $(k_c, 0, 0) = (1, 0, 0)$ yields

$$\hat{a} = -4, \quad \hat{b} = \frac{4}{3}, \quad \hat{c} = -6 \quad \text{and} \quad \lambda_3 = -3.$$

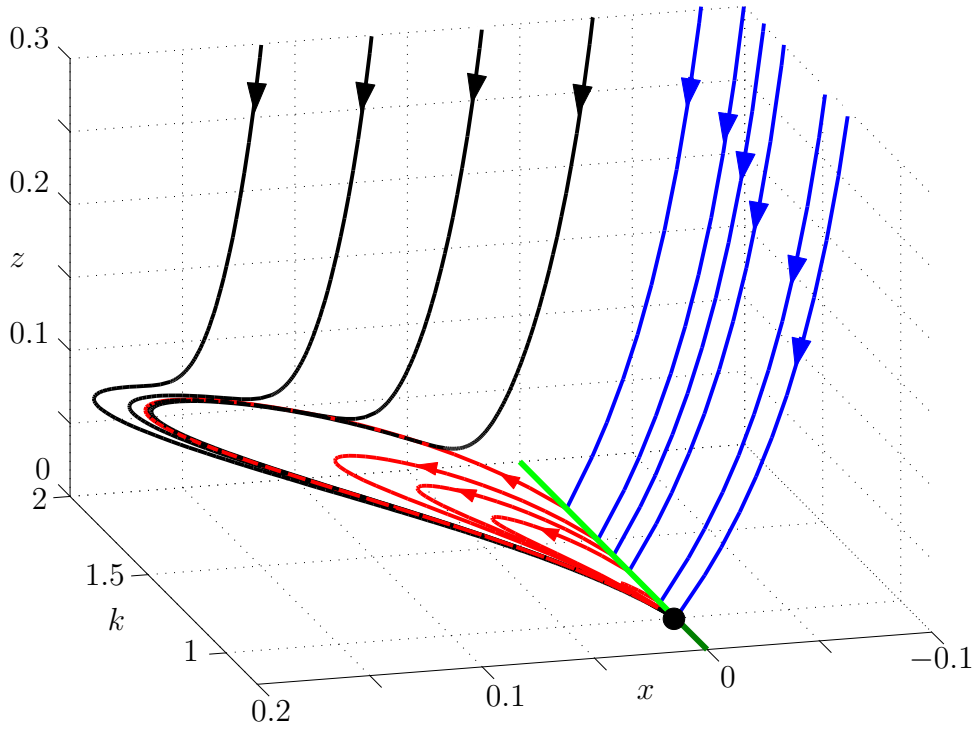

Figure 8: The phase portrait of system (34) for $\theta^* = 2$. The equilibrium $(k, 0, 0) = (1, 0, 0)$ has a three-dimensional basin of attraction due to a single-wedge bifurcation and is a BPB; see Fig. 1 for an explanation of the colours.

Hence, all conditions for a single-wedge bifurcation are satisfied.

Figure 8 displays the local dynamics near the bad point $(k_c, 0, 0) = (1, 0, 0)$. The behaviour near the k-axis is determined by the linearization (28). For our choice of parameters, this leads to

$$\left[\begin{array}{c|cc} 0 & 0 & 0 \\ \hline 0 & k-2 & 1 \\ 0 & k(4-k)-1 & -2 \end{array}\right]$$

with trace $k - 4$ and determinant $k^2 - 6k + 5$. Hence, all equilibria $(k, 0, 0)$ with $1 < k < 5$ are saddles with one-dimensional strong stable (blue) and one-dimensional strong unstable manifolds (red). Figure 8 shows only one branch of each of these strong manifolds. Both branches of the strong stable manifolds are unbounded, while both branches of the strong unstable manifolds form heteroclinic connections with other equilibria on the k-axis. The branches illustrated in Fig. 8 all converge to the *same* equilibrium point, namely the bad point $(1, 0, 0)$. All equilibria $(k, 0, 0)$ with $k < 1$ are stable and attract a two-dimensional (unbounded) subset of points (not illustrated). For k relatively close to 1 both eigenvalues are real and distinct. These equilibria have one-dimensional strong

stable manifolds similar to those of the saddles. The black curves in Fig. 8 are trajectories in the basin of attraction of the bad point. There exists a three-dimensional set of initial conditions whose trajectories behave like the ones illustrated, namely they quickly drop down or move up to the curved surface of heteroclinic connections and then converge to $(1, 0, 0)$. We are unable to calculate the exact boundaries of the basin of attraction of the bad point. It is bounded by the strong stable manifolds of the saddles and by a curved surface that is transverse to the heteroclinic connection of the saddle $(k, 0, 0)$ with $k \approx 1.6$. The strong unstable manifolds of the saddles with $k > 1.6$ do not converge to the bad point but to equilibria with $k < 1$.

Note that the other solution for Eq. (29) leads to the critical point $(k_c, 0, 0) = (5, 0, 0)$ which does not satisfy Eq. (30), that is, $k_c - 4 > 0$. Hence, this critical point only attracts a set that has zero measure in $\mathbb{R}^3$ and it is not a BP.

This example shows that in the $2+1$ case the value of the unknown parameter θ^* influences the stability type of the equilibria along the $k-$axis, as well as the global behaviour of the closed-loop system. For example, if $-4 - 2\sqrt{5} < \theta^* < -4 + 2\sqrt{5}$, then no real solution for k_c exists and there is no transcritical bifurcation.

3.2 Hopf bifurcation without parameters

If the two eigenvalues of the matrix A in Eq. (28) are purely imaginary, a Hopf bifurcation occurs. This is the case if $\operatorname{trace} A = 0$ and $\det A > 0$, that is,

$$\varphi_1 \, k_\infty - \mu_1 - \nu_1 = 0 \tag{35}$$

and

$$\begin{aligned} \varphi_1^2 \, k_\infty^2 - (\mu_1 + \nu_1 + \theta^* \, \varphi_1) \; \varphi_1 \, k_\infty + \mu_1 \, \nu_1 + 1 \;\; &> \;\; 0 \Leftrightarrow \\ \mu_1 \, \nu_1 + 1 - \theta^* \, \varphi_1 \, (\mu_1 + \nu_1) \;\; &> \;\; 0, \end{aligned} \tag{36}$$

where we used $\varphi_1 \, k_\infty = \mu_1 + \nu_1$ as required by Eq. (35). Hence, the critical point is at $k_\infty = k_H := \frac{\mu_1 + \nu_1}{\varphi_1}$, provided $\varphi_1 \neq 0$. The eigenvalues at the Hopf bifurcation are the purely imaginary complex conjugate pair $\lambda_{2,3} = \pm \omega \, i$ with

$$\omega^2 = \mu_1 \, \nu_1 + 1 - \theta^* \, \varphi_1 \, (\mu_1 + \nu_1). \tag{37}$$

The Hopf bifurcation in this context has been studied in [16] where the authors described the behaviour in normal form on a three-dimensional centre manifold. The closed-loop system (27) near a critical point $(k_H, 0, 0)$ can be brought in normal form by shifting the critical point to the origin ($K = k - k_H$) and using the transformation that brings the linear part into Jordan normal form, namely

$$\begin{pmatrix} K \\ x \\ z \end{pmatrix} = \begin{bmatrix} 1 & 0 & 0 \\ 0 & 1 & 0 \\ 0 & \mu_1 - \varphi_1 \, k_H & \omega \end{bmatrix} \begin{pmatrix} K \\ v \\ w \end{pmatrix} = \begin{bmatrix} 1 & 0 & 0 \\ 0 & 1 & 0 \\ 0 & -\nu_1 & \omega \end{bmatrix} \begin{pmatrix} K \\ v \\ w \end{pmatrix},$$

with $\omega > 0$ defined in (37). Following the calculations in [16], this leads to the normal form

$$\left\{\begin{array}{rcrcrcl} \dot{K} &=& \beta_{20}\, v^2 &+& \beta_{02}\, w^2 + \pi_{12}\, K\, v^2 + \rho_{12}\, K\, w^2 &+& \text{h.o.t,} \\ \dot{v} &=& \omega\, w &&&+& \text{h.o.t,} \\ \dot{w} &=& -\omega\, v &+& \zeta_{11}\, K\, v - \xi_{11}\, K\, w &&\\ &&&+& \alpha_{30}\, v^3 + \alpha_{21}\, v^2\, w + \alpha_{12}\, v\, w^2 + \alpha_{03}\, w^3 &&\\ &&&+& \zeta_{21}\, K^2\, v + \xi_{21}\, K^2\, w &+& \text{h.o.t.} \end{array}\right. \tag{38}$$

Here $\omega > 0$ is given by (37), and the other coefficients $\zeta_{11}, \ldots$, $\xi_{11}, \ldots$, $\alpha_{30}, \ldots$, $\beta_{20}, \ldots$, $\pi_{12}, \ldots$ and $\rho_{12}, \ldots$ depend on the coefficients for the expansions of φ, μ and ν and the unknown parameter θ^*. The qualitative behaviour of this system has been analysed in [16], where it is shown that the behaviour of Eq. (38) is determined by the sign of

$$(\beta_{20} + \beta_{02})\, \xi_{11} = \left(\frac{-\varphi_1\, B}{\nu_1^2 + \omega^2}\right) \left(-\varphi_1 \left[1 - \frac{\omega}{\nu_1^2 + \omega^2}\right]\right),$$

with

$$\begin{aligned} B &:= 1 + \nu_1\, (\nu_1 - \theta^*\, \varphi_1)\, (\omega + 1) \\ &= 1 + \frac{\nu_1}{\mu_1 + \nu_1}\, (\omega^2 - 1 + \nu_1^2)\, (\omega + 1). \end{aligned} \tag{39}$$

Again, $\omega > 0$ is defined in (37), which we used here to eliminate $\theta^*\, \varphi_1$. The sign of $(\beta_{20} + \beta_{02})\, \xi_{11}$ is the same as the sign of B, unless $\varphi_1 = 0$.

If $B > 0$, then the equilibria on the k-axis that lie to the left of the critical point are unstable, while those to the right of the critical point are stable. Here, initial conditions with a small negative K-coordinate near the equilibrium manifold spiral out such that K increases to a positive value; see also Fig. 2 (c). This is called the *elliptic* case in [5, 6, 7, 8]. Note that the cubic polynomial $(\omega^2 - 1 + \nu_1^2)\, (\omega + 1)$ has only one real root at $\omega = -1 < 0$ if $\nu_1 > 1$. Hence, we immediately see that B is always positive for $\omega > 0$ if $\nu_1 \geq 1$ (we assume $\mu_1 \geq 0$). If $\nu_1 < 1$, then the sign of B depends on θ^* and the choice for μ_1.

If $B < 0$, then the equilibria on the k-axis that lie to the left of the critical point are stable and the others unstable. In this case an invariant cone exists which acts as a separatrix for three qualitatively different behaviours. Solutions starting from initial conditions with $K < 0$ inside the invariant cone reach an equilibrium on the K-axis with $K < 0$. Solutions starting inside the cone with $K > 0$ show this behaviour in backward time and do not converge (locally) in forward time. Solutions starting from initial conditions outside the invariant cone first spiral inwards as long as $K < 0$ and then spiral outwards as soon as $K > 0$, so that again no convergence takes place locally; see also Fig. 2 (d). This is called the *hyperbolic* case in [5, 6, 7, 8]. Similar to the saddle-type transcritical bifurcation, the hyperbolic Hopf bifurcation can only occur in the context of

adaptive control if another critical point exist on the positive K-axis such that the equilibria to the right of this other critical point are again stable and attract the initial conditions that escape a neighbourhood of the Hopf point.

Both cases imply that the origin of Eq. (38), or equivalently the critical point $(k_H, 0, 0)$ of the original system (27), is a centre and the dynamics does not lead to a BP.

If $B = 0$, or if $\varphi_1 = 0$, then the three-jet (38) cannot determine the local behaviour around the critical point $(k_H, 0, 0)$ and higher-order analysis is required. If $\varphi_1 = 0$ then we must choose $\mu_1 = \nu_1 = 0$ in order to satisfy condition (35). Hence, one can easily design the adaptive controller such that this situation does not occur. Furthermore, $B = 0$ is possible only when $\nu_1 < 1$ (and $0 \leq \mu_1 \ll 1$. Then there are at most two values for ω at which $B = 0$, which corresponds to at most two values of θ^*, and we can consider this case as not typical, even in the context of adaptive back-stepping control. Moreover, it is always possible to design the adaptive controller such that the Hopf bifurcation is elliptic, independent of ω and thus θ^*. The analysis for these degenerate cases is beyond the scope of this paper.

As an example, we consider again the closed-loop system (34) of the previous section. Recall that

$$\varphi(x) = x, \quad \mu(x) = 2\,x \quad \text{and} \quad \nu(z) = 2\,z + 18\,z^2 + 41\,z^3,$$

and the closed-loop system is defined as

$$\begin{cases} \dot{k} &= -x^2 - (2+\theta^*)\,x\,z + k\,x\,z, \\ \dot{x} &= -2\,x + z + k\,x, \\ \dot{z} &= -x - 2\,z - 18\,z^2 - 41\,z^3 + (2+\theta^*)\,k\,x - k^2\,x. \end{cases}$$

Hence, potentially a Hopf bifurcation without parameters takes place on the k-axis at $k = k_H = \frac{\mu_1+\nu_1}{\varphi_1} = 4$. That is, $k_H = 4$ satisfies condition (35). Condition (36) is satisfied as well if θ^* is such that

$$\omega^2 = \mu_1\,\nu_1 + 1 - \theta^*\,\varphi_1\,(\mu_1 + \nu_1) = 5 - 4\,\theta^* > 0 \Leftrightarrow \theta^* < \frac{5}{4}.$$

Since $\nu_1 > 1$, the Hopf bifurcation without parameters, if it exists, is elliptic. Indeed, Eq. (39) becomes

$$B = 1 + \frac{1}{2}\,(\omega^2 + 3)\,(\omega + 1),$$

which is positive independent of ω and thus θ^*.

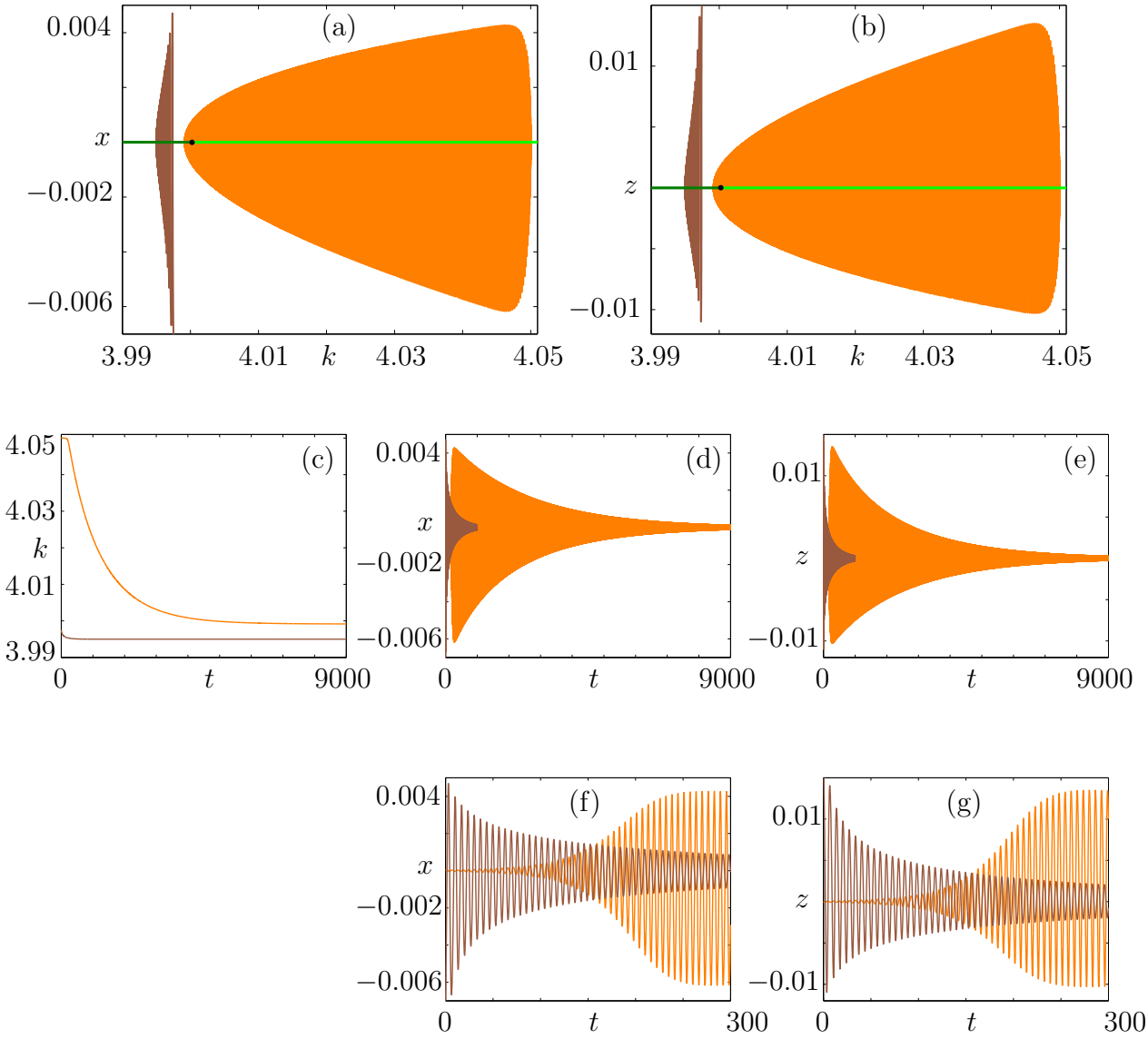

Figure 9: Dynamics near the Hopf bifurcation at $(k, 0, 0) = (4, 0, 0)$ for (34) with $\theta^* = 1$. Panels (a) and (b) show projections of two trajectories, one starting just before and one just after the Hopf point, onto the (k, x)-plane and the (k, z)-plane, respectively. Both trajectories spiral around the k-axis and converge to an equilibrium on the k-axis with k-value less than the value at $t = 0$. Panels (c), (d) and (f) show the time series up to $t = 9000$ for the coordinates k, x and z, respectively. The oscillations can be seen better in the enlargements (f) and (g) showing the time series up to $t = 300$ for x and z, respectively.

Let us study this system in more detail for $\theta^* = 1 < \frac{5}{4}$. The dynamics for $\theta^* = 1$ locally near $(k_H, 0, 0) = (4, 0, 0)$ is as shown in Fig. 2(c). Figure 9 shows the behaviour of two typical trajectories, one starting just before and one just after the critical point. Each trajectory spirals around the k-axis. For the trajectory starting just after the Hopf point the amplitude increases sharply, before dampening out to zero at an equilibrium to the left of the Hopf point. The amplitude of the trajectory starting just before the Hopf point decreases monotonically and the trajectory converges to an equilibrium with k-value less than where it started from. This behaviour is best seen in the time series of Fig. 9 (c)-(e). Figure 9 (c) shows that both trajectories are monotonically decreasing in k. The frequency of the oscillations is extremely high, so Figs. 9 (f) and 9(g) show the time series up to $t = 300$ for x and z, respectively, where the oscillating motion is now clearly visible.

The spiralling motion that is characteristic for the elliptic Hopf bifurcation without parameters only exists very close to $(4, 0, 0)$. Globally, the dynamics is organized by two transcritical bifurcation points on the k-axis that both lie to the left of the Hopf point. In contrast to the situation for $\theta^* = 2$, the direction transverse to the centre manifold is attracting for both critical points. Using the formulae in Sec. 3.1, one can easily check that $T_{\rm s} := (\frac{1}{2}[5 + \sqrt{5}], 0, 0)$ is of saddle type and $T_{\rm c} := (\frac{1}{2}[5 - \sqrt{5}], 0, 0)$ is a semi-centre.

The global dynamics for $\theta^* = 1$ is illustrated in Fig. 10. Most trajectories converge to an equilibrium to the left of $T_{\rm c}$. There is a neighbourhood near the Hopf point, which is not illustrated in the figure, where trajectories accumulate on equilibria in between $T_{\rm s}$ and the Hopf point. Figures 9 (a) and (b) are enlargements of the Hopf point shown in Figs. 10 (b) and (c).

Figure 11 shows the dynamics near the semi-centre $T_{\rm c}$. As expected, equilibria just to the right of $T_{\rm c}$ have one-dimensional strong unstable manifolds that form heteroclinic connections with equilibria to the left of $T_{\rm c}$. Four such heteroclinic connections are shown in different shades of blue and purple. The light-rose trajectory, which starts relatively far to the right of $T_{\rm c}$ is also a heteroclinic connection, but its behaviour is qualitatively different from the others. Namely, this trajectory is spiralling around the k-axis as it converges to an equilibrium; this oscillating behaviour is visible in the time series in Figs. 11 (c) and (d), where the x- and z-coordinate are plotted versus t, respectively. As was the case near the Hopf point, the k-coordinates of all trajectories decrease monotically.

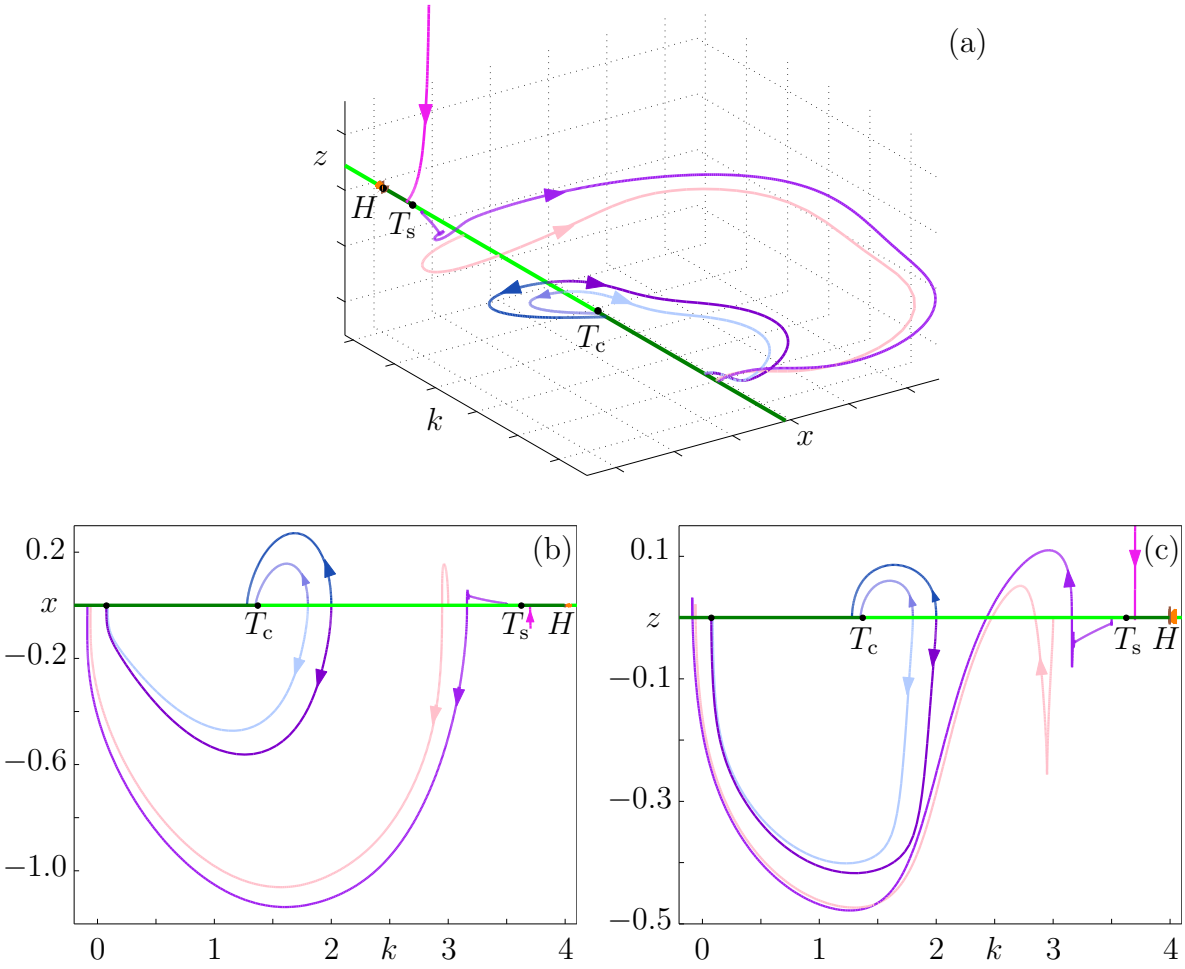

Figure 10: Global phase portrait of system (34) with $\theta^* = 1$. There are three critical points on the line of equilibria, namely a Hopf point (H), a saddle transcritical point (T_s) and a semi-centre transcritical point (T_c). An impression of the global behaviour is given in panel (a) with corresponding projections onto the (k, x)-plane (b) and the (k, z)-plane (c). All trajectories shown are discussed separately in Figs. 9, 11, and 12.

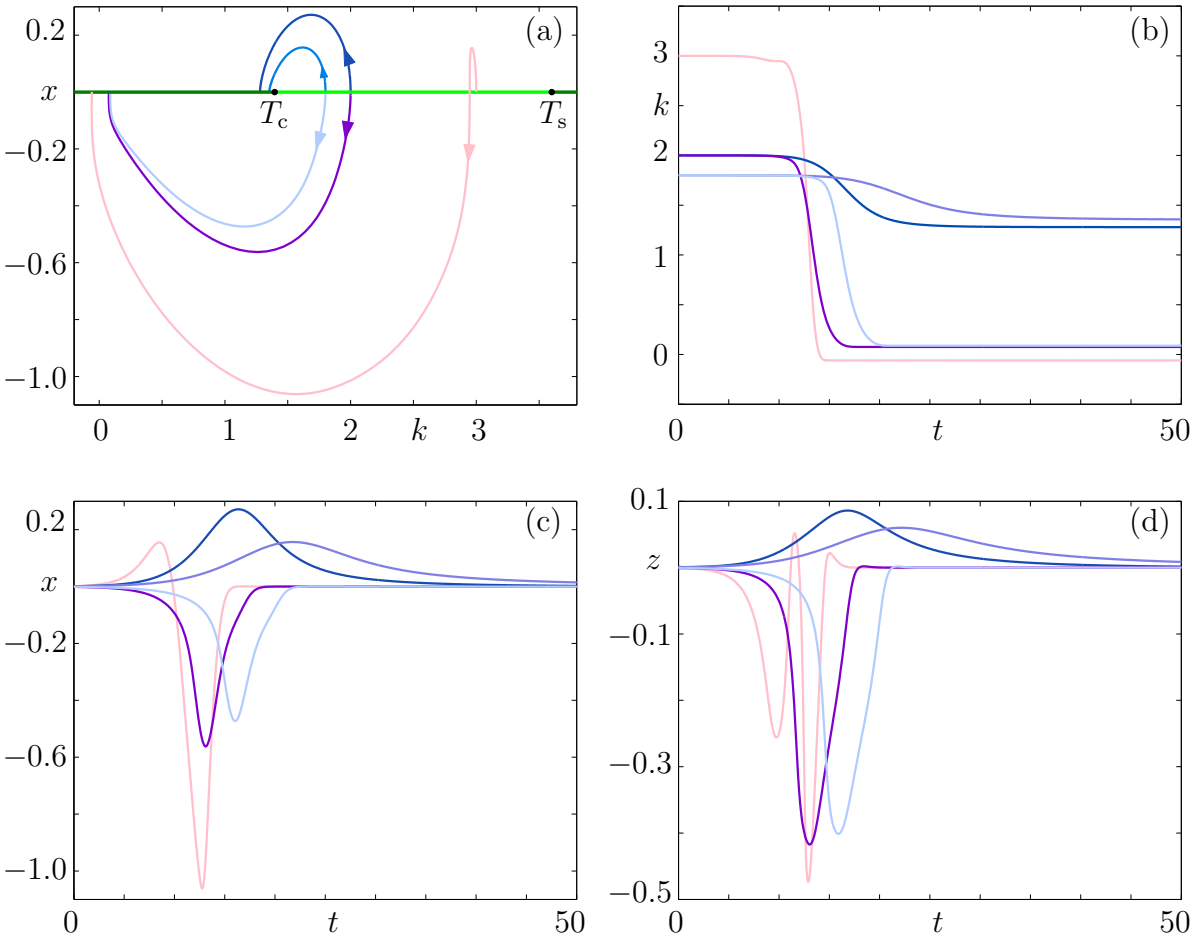

Figure 11: Dynamics near the semi-centre transcritical bifurcation at $(k, 0, 0) = (\frac{1}{2}[5 - \sqrt{5}], 0, 0)$ (T_c) for (34) with $\theta^* = 1$. Panel (a) shows five trajectories in phase space projected onto the (k, x)-plane. The behaviour of these five trajectories is further illustrated with the time series up to $t = 50$ in panels (b)-(d) for the coordinates k, x and z, respectively.

Figure 12 shows time series of the light-purple and magenta trajectories in Fig. 10. The magenta trajectory starts in between T_s and the Hopf point. Its k-coordinate drops only slightly and the x- and z-coordinates quickly converge to 0. The convergence happens in a spiralling motion around the k-axis, as shown in Figs. 12 (d) and (e). The light-purple trajectory starts just to the left of T_s. At first, this trajectory seems to diverge away from the k-axis, as is expected near a saddle transcritical point; see also Figs. 12 (d) and (e). Here, k is monotonically decreasing slowly. As soon as the trajectory has left a neighbourhood of T_s, it starts to behave similar to the light-rose trajectory depicted in detail in Fig. 11. Indeed, k decreases sharply until it comes close to its limiting value and the trajectory starts to spiral with relatively large amplitude before converging to an equilibrium to the left of T_c.

3.3 Bifurcations with respect to the unknown parameter

In the previous two sections we discussed the transcritical and Hopf bifurcations in the context of adaptive back-stepping control for the $2+1$ case, that is, with two variables and one unknown parameter θ^*. For this case the position of the critical points on the k-axis depends on θ^* and in this section we investigate these bifurcations in the (k_∞, θ^*)-plane in more detail.

As noted in Sec. 3.1, if $\varphi_1 = 0$, then no transcritical bifurcation exists on the k-axis. Furthermore, the Hopf bifurcation can only take place if $\mu_1 = \nu_1 = 0$ in which case the Hopf bifurcation is degenerate. Hence, we assume $\varphi_1 \neq 0$ and without loss of generality we choose $\varphi_1 = 1$ from now on.

The transcritical bifurcation takes place along a curve in the (k_∞, θ^*)-plane defined by condition (29)

$$\begin{aligned} k_\infty^2 - (\mu_1 + \nu_1 + \theta^*)\, k_\infty + \mu_1\,\nu_1 + 1 = 0 \quad &\Leftrightarrow \\ \theta^* = k_\infty - (\mu_1 + \nu_1) + \frac{\mu_1\,\nu_1 + 1}{k_\infty} \quad &\Leftrightarrow \\ \theta^* = k_\infty - \alpha^2 + \frac{\beta^2}{k_\infty}, \qquad &(40) \end{aligned}$$

for parameters $\alpha > 0$ and $\beta > 0$ with

$$\begin{aligned} \alpha^2 &= \mu_1 + \nu_1 \quad \text{and} \\ \beta^2 &= \mu_1\,\nu_1 + 1. \end{aligned}$$

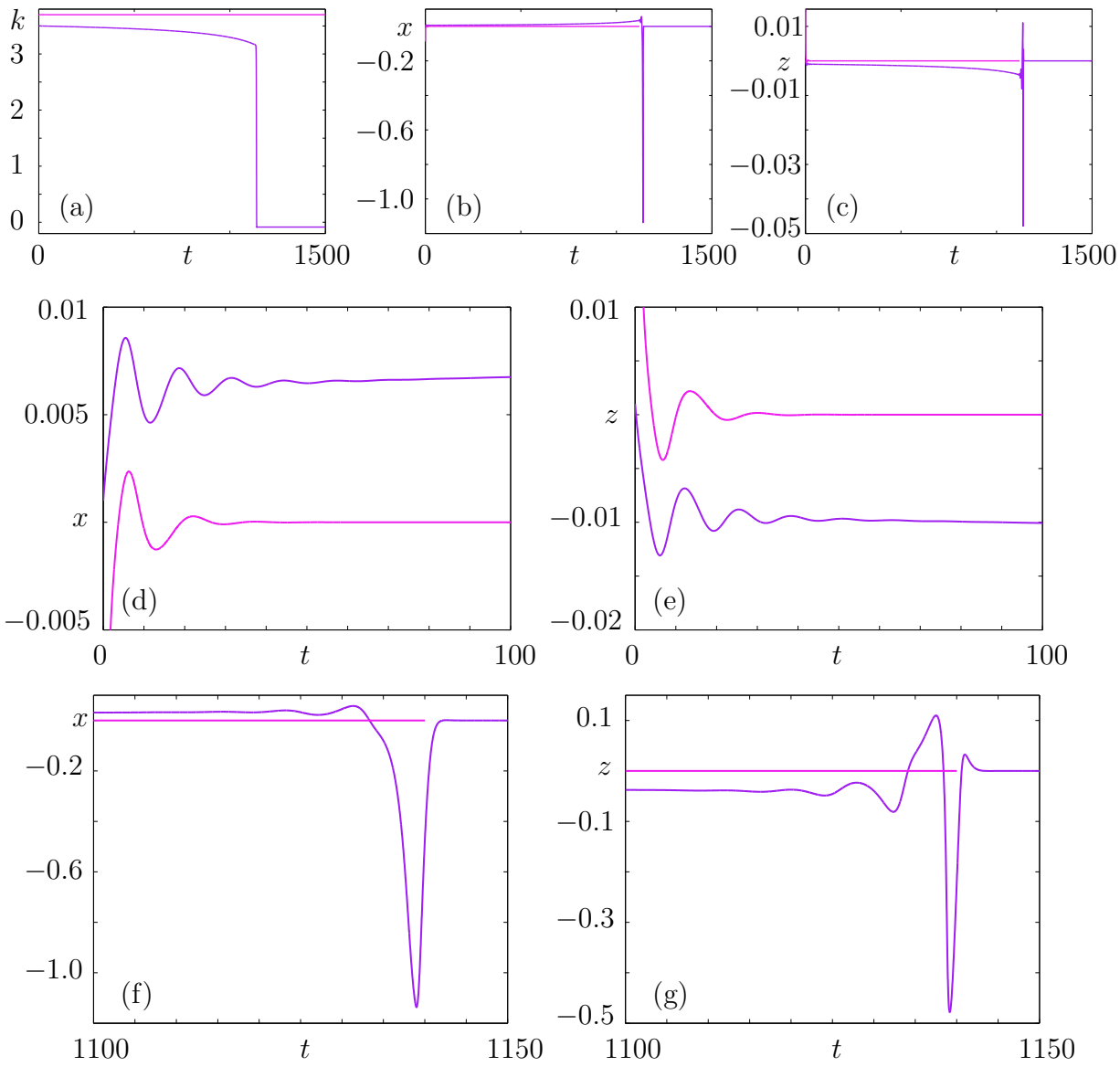

Figure 12: Time series up to $t = 1500$ of two trajectories near the saddle transcritical bifurcation at $T_s = (\frac{1}{2}[5 + \sqrt{5}], 0, 0)$ for (34) with $\theta^* = 1$. Panels (a)-(c) show the k-, x- and z-coordinates, respectively. Enlargements for the x- and z-coordinates are shown up to $t = 100$ in panels (d) and (e) and for $1100 \leq t \leq 1150$ in panels (f) and (g), respectively.

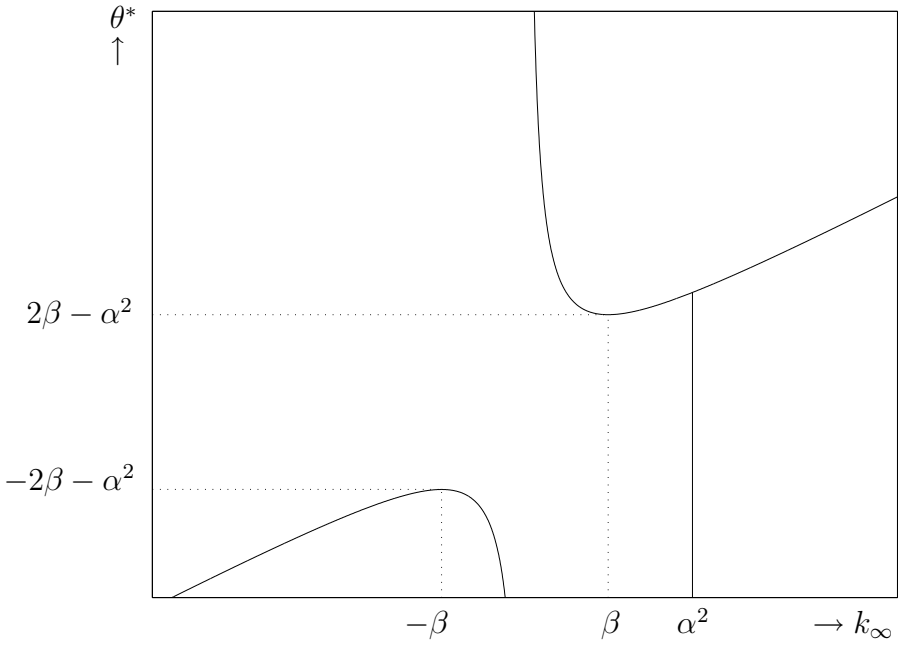

Figure 13: The bifurcation diagram in the (k_∞, θ^*)-plane with $\alpha^2 > \beta$.

The curve defined by Eq. (40) has a local maximum at $(k_\infty, \theta^*) = (-\beta, -2\,\beta - \alpha^2)$ and a local minimum at $(k_\infty, \theta^*) = (\beta, 2\,\beta - \alpha^2)$. A sketch of this curve is shown in Fig. 13. Recall that the transcritical bifurcation only makes sense in the context of adaptive back-stepping control if condition (30) is satisfied as well, which amounts to $k_\infty < \alpha^2$.

The Hopf bifurcation is defined by Eq. (35)

$$k_\infty = \frac{\mu_1 + \nu_1}{\varphi_1} \Leftrightarrow k_\infty = \alpha^2, \tag{41}$$

where we again assume $\varphi_1 = 1$. Additionally, we must satisfy condition (36), that is,

$$\theta^* < \frac{\mu_1\,\nu_1 + 1}{\varphi_1\,(\mu_1 + \nu_1)} = \frac{\beta^2}{\alpha^2}.$$

Here we assume $\alpha \neq 0$. This curve is shown in Fig. 13 for the case $\alpha^2 > \beta$.

The two curves (40) and (41) intersect at the point

$$(k_\infty, \theta^*) = \left(\frac{\mu_1 + \nu_1}{\varphi_1},\ \frac{\mu_1\,\nu_1 + 1}{\varphi_1\,(\mu_1 + \nu_1)}\right) = \left(\alpha^2,\ \frac{\beta^2}{\alpha^2}\right).$$

As explained above, this intersection point does not correspond to a transcritical bifurcation in our context, and it also does not correspond to a Hopf bifurcation.

In fact, this point is a Bogdanov-Takens bifurcation point. The Bogdanov-Takens bifurcation is of codimension two and is not generic for the $2+1$ case. It would be generic only if there are at least two unknown parameters, i.e., $\theta^* \in \mathbb{R}^2$. The possible dynamics near a critical point of this type can be quite complicated and the details for the $2+1$ case are left for future work; see [6] for a discussion of the Bogdanov-Takens bifurcation without (two) parameters in the general context of dynamical systems theory.

Figure 13 shows that θ^* can have a dramatic influence on the dynamics of the closed-loop system (27). For example, if $\theta^* < -2\,\beta - \alpha^2$ then there are three critical points on the equilibrium manifold. Two of these points are transcritical bifurcation points, and the third at $(\alpha^2, 0, 0)$ is a Hopf point. For $\theta^* \in (-2\,\beta - \alpha^2, 2\,\beta - \alpha^2)$ only a Hopf bifurcation (without parameters) exists. For $\theta^* \in (2\,\beta - \alpha^2, \beta^2/\alpha^2)$ the situation is similar as for $\theta^* < -2\,\beta - \alpha^2$, but if $\theta^* > \beta^2/\alpha^2$ then there is only one transcritical bifurcation point that corresponds to a stabilized system. For example, the closed-loop system (34) gives $\alpha^2 = 4$ and $\beta^2 = 5$, such that $2\,\beta - \alpha^2 = 2\sqrt{5} - 4 \approx 0.47$ and $\beta^2/\alpha^2 = 5/4$, which leads to three critical points ordered as shown in Fig. 10 for $\theta^* = 1$.

Let us now investigate the local dynamics near the critical points along these bifurcation curves. Along the transcritical bifurcation curve a segment may correspond to a curve of single-wedge bifurcations. This is the case if conditions (33) are satisfied. From the definitions (32) for $\hat{a}$ and $\hat{b}$ we find

$$\begin{aligned} \hat{a} &= \frac{-\nu_1\,k_c^2 + 2\,\mu_1\,\nu_1\,k_c - \mu_1\,\beta^2}{k_c}, \\ \hat{b} &= -\frac{1}{\lambda_3}\,\frac{\beta^2 - k_c^2}{k_c}. \end{aligned}$$

First note that $k_c \neq 0$ along the curve of transcritical bifurcations. Furthermore,

$$(2\,\mu_1\,\nu_1)^2 - 4\,\mu_1\,\nu_1\,\beta^2 = -4\mu_1\,\nu_1 \leq 0$$

due to the definition of β. Hence, $\hat{a} < 0$ and in order to satisfy $\hat{a}\,\hat{b} < 0$, we must have $\hat{b} > 0$, which is equivalent to

$$-\beta < k_c < \beta,$$

since $\lambda_3 < 0$. This means, in particular, that the transcritical bifurcation points with $k_c < -\beta$ or $k_c > \beta$ are of saddle type. The transcritical bifurcation is of single-wedge type for $k_c \in (-\beta, \beta)$, provided $\hat{c}^2 + 4\,\hat{a}\,\hat{b} \geq 0$. Indeed, as shown in Figs. 10, 12 and 11, for system (34) with $\theta^* = 1$ we encounter a semi-centre transcritical bifurcation at $T_{\rm c}$ with $k_c = \frac{1}{2}\,[5 - \sqrt{5}] < \beta = \sqrt{5}$, a saddle transcritical bifurcation at $T_{\rm s}$ with $k_c = \frac{1}{2}\,[5 + \sqrt{5}] > \beta$ and a Hopf bifurcation at $k_c = 4 = \alpha^2$.

Along the Hopf bifurcation curve we must investigate the sign of B, given by (39), namely

$$B = 1 + \frac{\nu_1}{\mu_1 + \nu_1}\,(\omega^2 - 1 + \nu_1^2)\,(\omega + 1).$$

The associated θ^*-values are then

$$\theta^* = \frac{\beta^2 - \omega^2}{\alpha^2}.$$

Since B is positive for relatively large $\omega > 0$ (certainly for $\omega \geq \sqrt{1-\nu_1^2}$), all Hopf points for $\theta^* \leq 0$ will be elliptic. For $\theta^* > 0$, a short interval may exist along which the Hopf points are hyperbolic, depending on μ_1 and ν_1. Recall that this requires $0 \leq \nu_1 < 1$ and $0 \leq \mu_1 \ll 1$, so that it is easy to design an adaptive closed-loop system that avoids this situation.

Similar bifurcation diagrams can be obtained for the cases $\alpha^2 < \beta$ and $\alpha^2 = \beta$, and when $\varphi_1 < 0$.

4 Discussion

In this paper we investigated the behaviour of uncertain closed-loop systems that were obtained using adaptive back-stepping control. Such closed-loop systems are $(n+p)$-dimensional, where the first n equations describe the evolution of the state $x \in \mathbb{R}^n$ and the next p equations describe the adaptation of the estimate to an unknown parameter $\theta^* \in \mathbb{R}^p$. The controller is designed such that the state x is stabilized, that is, the origin is a global attractor (independent of θ^*). This leads to a p-dimensional equilibrium manifold that consists entirely of equilibria, each of which has at least one eigenvalue on the imaginary axis. Critical points on the equilibrium manifold, that is, points with more than one eigenvalue on the imaginary axis are considered bifurcation points and their existence leads to the notion of so-called bifurcations without parameters.

We considered the cases $1+1$ and $2+1$ in great detail. In particular, we were interested in so-called bad point bifurcations, where the closed-loop system is in a sense unstable because the adaptation can never be frozen such that the associated closed-loop system is stabilized. Bad point bifurcations may occur at critical points. Critical points for the 1+1 case are always transcritical bifurcation points. We found that bad behaviour arises from a single-wedge bifurcation which occurs for many choices of the adaptive controller. Indeed, for the $1+1$ case it is hard to avoid the single-wedge bifurcation and the resulting controller is not robust under small variations of the underlying system. As mentioned in Sec. 2.5, the controller can be designed to robustly avoid the single-wedge bifurcation if one introduces an extra parameter ϱ in the equation for the adaptation.

For the $2+1$ case, the typical critical points on the equilibrium manifold are either transcritical or Hopf points. Here, the type of the bifurcation depends on the unknown parameter θ^* and may vary as θ^* varies. For large ranges of θ^* the adaptive controller is robust and bad behaviour can be avoided.

We consider the behaviour of the $2+1$ closed-loop system as typical for the general $n+1$ case. If $n > 2$, then still only transcritical and Hopf bifurcations

occur typically and the dynamics can be examined by centre manifold reduction. In the context of adaptive control, we require the additional property that the centre manifold be attracting.

If more than one parameter is unknown, i.e. $p > 1$, then the dynamics can become much more complicated. For the particular case with $n = 1$ the equilibrium manifold separates the $(1 + p)$-dimensional state space of the closed-loop system and we find no other types of bad behaviour. However, if also $n > 1$, then bifurcations without parameters of higher codimension are possible. We restricted our study to codimension-one bifurcations and the general case $n + p$ with both $n > 1$ and $p > 1$ is left for future research.

References

[1] Aamo, O. M. & Krstić, M. [2003] *Flow Control By feedback; stabilization and mixing* Communications and Control Engineering Series (Springer-Verlag London Ltd., London).

[2] Astrom, K. J. & Wittenmark, B. [1995] *Adaptive Control* (Adison-Wesley), 2nd edition.

[3] Back, A., Guckenheimer, J., Myers, M. R., Wicklin, F. J. & Worfolk, P. A. [1992] "Dstool: Computer assisted exploration of dynamical systems," *Notices Amer. Math. Soc.*, **39**(4), 303–309.

[4] Dumortier, F. & Roussarie, R. [2000] "Geometric singular perturbation theory beyond normal hyperbolicity," in *Multiple-time-scale dynamical systems*, IMA Volumes in Mathematics and its Applications Vol. 122, eds. Jones, C. K. R. T. & Khibnik, A. I. (Springer-Verlag, New York).

[5] Fiedler, B. & Liebscher, S. [2000] "Generic Hopf bifurcation from lines of equilibria without parameters: II. Systems of viscous hyperbolic balance laws," *SIAM J. Math. Anal.* **31**(6), 1396–1404.

[6] Fiedler, B. & Liebscher, S. [2001] "Takens-Bogdanov bifurcations without parameters and oscillatory shock profiles," in *Global analysis of dynamical systems*, eds. Broer, H. W., Krauskopf, B. & Vegter, G. (Institute of Physics Publishing, Bristol), pp. 211–259.

[7] Fiedler, B., Liebscher, S. & Alexander, J. C. [2000] "Generic Hopf bifurcation from lines of equilibria without parameters: I. Theory," *J. Differential Equations* **167**(1), 16–35.

[8] Fiedler, B., Liebscher, S. & Alexander, J. C. [2000] "Generic Hopf bifurcation from lines of equilibria without parameters: III. Binary oscillations," *Int. J. Bifurcation and Chaos* **10**(7), 1613–1621.

[9] Guckenheimer, J. & Holmes, P. [1990] *Nonlinear oscillations, dynamical systems, and bifurcations of vector fields* (Springer-Verlag, New York), 2nd edition.

[10] Ioannou, P. A. & Sun, J. [1996] *Robust adaptive control* (Prentice Hall Inc., Upper Saddle River NJ).

[11] Isidori, A. [1995] *Nonlinear control systems* (Springer-Verlag, London), 3rd edition.

[12] Khalil, H. K. [1992] *Nonlinear systems* (Macmillan, New York).

[13] Krstić, M., Kanellakopoulos, I. & Kokotović, P. V. [1992] "Adaptive nonlinear control without overparametrization," *Systems Control Lett.* **19**(3), 177–185.

[14] Krstić, M. [1996] "Invariant manifolds and asymptotic properties of adaptive nonlinear stabilizers," *IEEE Trans. Automat. Control* **41**(6), 817–829.

[15] Kuznetsov, Y. A. [1998] *Elements of applied bifurcation theory* (Springer-Verlag, New York), 2nd edition.

[16] Leach, J. A., Triantafillidis, S., Owens, D. H. & Townley, S. [1995] "The dynamics of universal adaptive stabilization: computational and analytical studies," *Control Theory Adv. Tech.* **10**(4, part 4), 1689–1716.

[17] Mestel, B. D. & Townley, S. [1993] "Topological classification of universal adaptive dynamics," in *Proc. 2nd European Contr. Conf.*, eds. Nieuwenhuis, J. W., Praagman, C. & Trentelman, H. L. (Groningen, the Netherlands).

[18] Osinga, H. M. & Rokni Lamooki, G. R. [2000] "One-dimensional strong stable and unstable manifolds code," extension module for the tcl/tk version of DsTool; available via `http://www.enm.bris.ac.uk/staff/hinke/dss/ode/ssman1d/`.

[19] Sontag, E. D. [1998] *Mathematical control theory.* (Springer-Verlag, New York), 2nd edition.

[20] Townley, S. [1996] "Topological aspects of universal adaptive stabilization," *SIAM J. Control Optim.* **34**(3), 1044–1070.

[21] Townley, S. [1999] "An example of a globally stabilizing adaptive controller with a generically destabilizing parameter estimate," *IEEE Trans. Automat. Control* **44**(11), 2238–2241.

A Construction of the controller in the $2{+}1$ case

Consider the two-dimensional system in strict feedback form

$$\begin{cases} \dot{x} &= y + \theta^* \varphi(x), \\ \dot{y} &= u, \end{cases}$$

with state variables $x, y \in \mathbb{R}$, control $u \in \mathbb{R}$ and unknown parameter $\theta^* \in \mathbb{R}$. The adaptive back-stepping controller is constructed in two steps.

First we focus on the $x-$equation only and regard y as the control. As before, we work with a Lyapunov function $V_1 = \frac{1}{2}(x^2 + k^2)$, where $k = \theta^* - \hat{\theta}$ is the error between the true value θ^* and the estimation $\hat{\theta}$ of the unknown parameter. The x-equation is stabilized if $\dot{V}_1 < 0$ for all $x \neq 0$. We have

$$\begin{aligned} \dot{V}_1 &= x\,\dot{x} + k\,\dot{k} \\ &= x\,(y + \theta^*\,\varphi(x)) + k\,(-\dot{\hat{\theta}}) \\ &= x\,(y + \hat{\theta}\,\varphi(x)) + k\,(x\,\varphi(x)) - \dot{\hat{\theta}}). \end{aligned}$$

In the same manner as for Example 1 in Sec. 1, we stabilize the x-equation using

$$y = -\mu(x) - \hat{\theta}\,\varphi(x) \quad \text{and} \quad \dot{\hat{\theta}} = x\,\varphi(x),$$

where μ is an arbitrary function such that $\mu(0) = 0$ and $x\,\mu(x) > 0$ for all $x \neq 0$.

Since $\dot{y} = u$, it is now tempting to set $u = \frac{dy}{dt} = \frac{d}{dt}\left(-\mu(x) - \hat{\theta}\,\varphi(x)\right)\hat{\theta}$. Unfortunately, even though this would stabilize x, we cannot guarantee $y \to 0$ as $t \to \infty$. The actual controller must be such that both x and y are stabilized. Using $\mu(0) = \varphi(0) = 0$, this will be achieved if

$$\left\| y - \left[-\mu(x) - \hat{\theta}\,\varphi(x)\right] \right\| \to 0 \quad \text{as} \quad t \to \infty.$$

Let us introduce the notation $z = y + \mu(x) + \hat{\theta}\,\varphi(x)$ and rewrite the equations to

$$\dot{x} = y + \theta^*\,\varphi(x) = z - \mu(x) + k\,\varphi(x)$$

and

$$\begin{aligned} \dot{z} &= \frac{d}{dt}(y + \mu(x) + \hat{\theta}) \\ &= u + \frac{d}{dx}\mu(x)\,\dot{x} + \left(\frac{d}{dx}\varphi(x)\,\dot{x}\right)\,\hat{\theta} + \varphi(x)\,\dot{\hat{\theta}}. \end{aligned}$$

We now proceed in the same manner as before, but use the Lyapunov function $V = \frac{1}{2}\,(x^2 + z^2 + k^2)$. After some algebraic manipulation, we obtain

$$\begin{aligned} \dot{V} &= x\,\dot{x} + z\,\dot{z} + k\,\dot{k} \\ &= -x\,\mu(x) + z\left[u + x + \left(\frac{d}{dx}\mu(x) + \frac{d}{dx}\varphi(x)\,\hat{\theta}\right)\,[-\mu(x) + z] + \varphi(x)\,\dot{\hat{\theta}}\right] \\ &\quad + k\left[x\,\varphi(x) + z\,\left(\frac{d}{dx}\mu(x) + \frac{d}{dx}\varphi(x)\,\hat{\theta}\right)\,\varphi(x) - \dot{\hat{\theta}}\right]. \end{aligned}$$

We wish to have u and $\dot{\hat{\theta}}$ such that

$$\dot{V} = -x\,\mu(x) - z\,\nu(z),$$

for some arbitrary functions μ and ν with $\mu(0) = 0$, $\nu(0) = 0$ and $x\,\mu(x) > 0$, $z\,\nu(z) > 0$ for all $x \neq 0$ and $z \neq 0$. To this end, we choose

$$u = -\nu(z) - x - \left(\frac{d}{dx}\mu(x) + \frac{d}{dx}\varphi(x)\,\hat{\theta}\right)\,[-\mu(x) + z] - \varphi(x)\,\dot{\hat{\theta}}$$

and

$$\dot{\hat{\theta}} = \varphi(x)\,\left[x + z\,\left(\frac{d}{dx}\mu(x) + \frac{d}{dx}\varphi(x)\,\hat{\theta}\right)\right].$$

Note that the actual adaptation law is a modification of $\dot{\hat{\theta}} = x\,\varphi(x)$, which yields a controller that stabilizes $(x, y) = (0, 0)$. Hence, the closed-loop system becomes

$$\left\{\begin{array}{rcl} \dot{k} &=& -\varphi(x)\,\left[x + z\,\left(\frac{d}{dx}\mu(x) + \frac{d}{dx}\varphi(x)\,[\theta^* - k]\right)\right], \\ \dot{x} &=& -\mu(x) + z + k\,\varphi(x), \\ \dot{z} &=& -x - \nu(z) + \left(\frac{d}{dx}\mu(x) + \frac{d}{dx}\varphi(x)\,[\theta^* - k]\right)\,k\,\varphi(x). \end{array}\right.$$

Using the same argument as in Sec. 2 it can be observed that for all initial conditions (k_0, x_0, z_0)

$$\lim_{t\to\infty} \|(x(t), z(t))\| = 0$$

and there exists $k_\infty \in \mathbb{R}$ depending on k_0, x_0 and z_0 such that $\lim_{t\to\infty} k(t) = k_\infty$. Hence, any initial condition (k_0, x_0, z_0) of the adaptive closed-loop system defines a non-adaptive limit controller

$$u = -\nu(z) - x - \left(\frac{d}{dx}\mu(x) + \frac{d}{dx}\varphi(x)\,(\theta^* - k_\infty\right)\,(-\mu(x) + z)\,.$$

Furthermore, the point $(x, z) = (0, 0)$ is always an equilibrium of the corresponding limit system

$$\left\{\begin{array}{rcl} \dot{x} &=& -\mu(x) + z + k_\infty\,\varphi(x), \\ \dot{z} &=& -x - \nu(z) + \left(\frac{d}{dx}\mu(x) + \frac{d}{dx}\varphi(x)\,(\theta^* - k_\infty\right)\,k_\infty\,\varphi(x), \end{array}\right.$$

because $\varphi(0) = \mu(0) = \nu(0) = 0$.

B Centre manifold reduction in the $2+1$ case

Let us assume that a transcritical bifurcation without parameters takes place on the k-axis of the closed-loop system

$$\left\{\begin{array}{rcl} \dot{k} &=& -\varphi(x)\,\left[x+z\,\left(\frac{d}{dx}\mu(x)+\frac{d}{dx}\varphi(x)\,[\theta^*-k]\right)\right],\\ \dot{x} &=& -\mu(x)+z+k\,\varphi(x),\\ \dot{z} &=& -x-\nu(z)+\left(\frac{d}{dx}\mu(x)+\frac{d}{dx}\varphi(x)\,[\theta^*-k]\right)\,k\,\varphi(x). \end{array}\right. \tag{42}$$

As before we assume that, in a neighbourhood of the k-axis, polynomial expansions of $\varphi(x)$, $\mu(x)$ and $\nu(z)$ exist up to large enough power, denoting their coefficients by φ_i, μ_i and ν_i, respectively. In what follows, we expand the functions $\varphi(x)$, $\mu(x)$ and $\nu(z)$ up to fourth order. Then the transcritical bifurcation is characterized, for some $k=k_c$, by Eqs. (29) and (30), that is,

$$\begin{array}{rcl} \varphi_1^2\,k_c^2-(\mu_1+\nu_1+\theta^*\,\varphi_1)\,\varphi_1\,k_c+\mu_1\,\nu_1+1 &=& 0,\\ \varphi_1\,k_c-\mu_1-\nu_1 &<& 0. \end{array}$$

As the first step, we shift the critical point $(k_c,0,0)$ to the origin via the coordinate transformation $K=k-k_c$. The equations now become

$$\begin{array}{rcl} \dot{K} &=& -\varphi_1\,x^2+(\varphi_1^2\,k_c-\tilde{\varphi}_1)\,x\,z\\ && -\varphi_2\,x^3+(3\,\varphi_1\,\varphi_2\,k_c-\tilde{\varphi}_2)\,x^2\,z+\varphi_1^2\,K\,x\,z\\ && -\varphi_3\,x^4-\tilde{\varphi}_3\,x^3\,z+3\,\varphi_1\,\varphi_2\,K\,x^2\,z+\cdots, \end{array} \tag{43}$$

$$\begin{array}{rcl} \dot{x} &=& (\varphi_1\,k_c-\mu_1)\,x+z\\ && +\varphi_1\,K\,x+(\varphi_2\,k_c-\mu_2)\,x^2\\ && +\varphi_2\,K\,x^2+(\varphi_3\,k_c-\mu_3)\,x^3\\ && +\varphi_3\,K\,x^3+(\varphi_4\,k_c-\mu_4)\,x^4+\cdots, \end{array} \tag{44}$$

and

$$\begin{array}{rcl} \dot{z} &=& (-1+\tilde{\varphi}_1\,k_c-\tilde{\psi}_1\,k_c^2)\,x-\nu_1\,z\\ && +(\tilde{\varphi}_1-2\,\tilde{\psi}_1\,k_c)\,K\,x+(\tilde{\varphi}_2-\tilde{\psi}_2\,k_c)\,k_c\,x^2-\nu_2\,z^2\\ && +(\tilde{\varphi}_2-2\,\tilde{\psi}_2\,k_c)\,K\,x^2+(\tilde{\varphi}_3-\tilde{\psi}_3\,k_c)\,k_c\,x^3-\nu_3\,z^3-\tilde{\psi}_1\,K^2\,x\\ && +(\tilde{\varphi}_3-2\,\tilde{\psi}_3\,k_c)\,K\,x^3+(\tilde{\varphi}_4-\tilde{\psi}_4\,k_c)\,k_c\,x^4-\nu_4\,z^4-\tilde{\psi}_2\,K^2\,x^2\\ && +\cdots, \end{array} \tag{45}$$

where

$$\begin{array}{rcl} \tilde{\varphi}_1 &=& \varphi_1\,(\mu_1+\theta^*\,\varphi_1),\\ \tilde{\varphi}_2 &=& \varphi_2\,(\mu_1+\theta^*\,\varphi_1)+2\,\varphi_1\,(\mu_2+\theta^*\,\varphi_2),\\ \tilde{\varphi}_3 &=& \varphi_3\,(\mu_1+\theta^*\,\varphi_1)+2\,\varphi_2\,(\mu_2+\theta^*\,\varphi_2)+3\,\varphi_1\,(\mu_3+\theta^*\,\varphi_3),\\ &\vdots& \end{array}$$

and

$$\begin{aligned}
\tilde{\psi}_1 &= \varphi_1\,\varphi_1 &&= \varphi_1^2,\\
\tilde{\psi}_2 &= \varphi_2\,\varphi_1 + 2\,\varphi_1\,\varphi_2 &&= 3\,\varphi_1\,\varphi_2,\\
\tilde{\psi}_3 &= \varphi_3\,\varphi_1 + 2\,\varphi_2\,\varphi_2 + 3\,\varphi_1\,\varphi_3 &&= 4\,\varphi_1\,\varphi_3 + 2\,\varphi_2^2,\\
\tilde{\psi}_4 &= \varphi_4\,\varphi_1 + 2\,\varphi_3\,\varphi_2) + 3\,\varphi_2\,\varphi_3 + 4\,\varphi_1\,\varphi_4 &&= 5\,\varphi_1\,\varphi_4 + 5\,\varphi_2\,\varphi_3.\\
&\vdots
\end{aligned}$$

In the next step, we apply a coordinate transformation such that the coordinate axes are the eigenspaces of the linearization. Recall that the linearization matrix is given by

$$\begin{bmatrix} 0 & 0 & 0 \\ 0 & -\mu_1 + \varphi_1\,k_c & 1 \\ 0 & -1 + \varphi_1\,(\mu_1 + \theta^*\,\varphi_1 - \varphi_1^2\,k_c^2 & -\nu_1 \end{bmatrix}.$$

Hence, the coordinate transformation is defined as

$$\begin{pmatrix} K \\ x \\ z \end{pmatrix} = \begin{bmatrix} 1 & 0 & 0 \\ 0 & 1 & 1 \\ 0 & \mu_1 - \varphi_1\,k_c & -\nu_1 \end{bmatrix} \begin{pmatrix} K \\ v \\ w \end{pmatrix}. \tag{46}$$

The transformation (46) leaves K invariant. Hence, the equation for K is easily obtained by substituting $v + w$ for x and $(\mu_1 - \varphi_1\,k_c)\,v - \nu_1 w$ for z in Eq. (43). Thus, up to second order, we get

$$\dot{K} = -\varphi_1\,(v+w)^2 + (\varphi_1^2\,k_c - \tilde{\varphi}_1)\,(v+w)\,([\mu_1 - \varphi_1\,k_c]\,v - \nu_1\,w). \tag{47}$$

The equations for v and w are given by

$$\begin{aligned}
\dot{v} &= -\frac{\nu_1}{\lambda_3}\,\dot{x} - \frac{1}{\lambda_3}\,\dot{z},\\
\dot{w} &= -\frac{\mu_1 - \varphi_1\,k_c}{\lambda_3}\,\dot{x} + \frac{1}{\lambda_3}\,\dot{z},
\end{aligned}$$

where $\lambda_3 = \varphi_1\,k_c - \mu_1 - \nu_1$. Using Eqs. (44) and (45) and after substituting $v + w$ for x and $(\mu_1 - \varphi_1\,k_c)\,v - \nu_1 w$ for z, we find

$$\begin{aligned}
\dot{v} &= \beta_{02}\,(v+w)^2 + \beta_{11}\,K\,(v+w) + \frac{\nu_2}{\lambda_3}\,([\mu_1 - \varphi_1\,k_c]\,v - \nu_1\,w)^2\\
&\quad + \beta_{03}\,(v+w)^3 + \beta_{12}\,K\,(v+w)^2 + \beta_{21}\,K^2\,(v+w)\\
&\quad + \frac{\nu_3}{\lambda_3}\,([\mu_1 - \varphi_1\,k_c]\,v - \nu_1\,w)^3 + \cdots,
\end{aligned} \tag{48}$$

where

$$\begin{aligned}
\beta_{0i} &= -\frac{1}{\lambda_3}\,(\nu_1\,(\varphi_i\,k_c - \mu_i) - \tilde{\psi}_i\,k_c^2 + \tilde{\varphi}_i\,k_c), && i \geq 2,\\
\beta_{1i} &= -\frac{1}{\lambda_3}\,(\nu_1\,\varphi_i + \tilde{\varphi}_i - 2\,\tilde{\psi}_i\,k_c), && i \geq 1,\\
\beta_{2i} &= \frac{1}{\lambda_3}\,\tilde{\psi}_i, && i \geq 1.
\end{aligned}$$

Similarly,

$$\begin{aligned}\dot{w} &= \lambda_3\, w \\ &\quad +\alpha_{02}\,(v+w)^2 + \alpha_{11}\,K\,(v+w) - \frac{\nu_2}{\lambda_3}\,([\mu_1-\varphi_1\,k_c]\,v-\nu_1\,w)^2 \\ &\quad +\alpha_{03}\,(v+w)^3 + \alpha_{12}\,K\,(v+w)^2 + \alpha_{21}\,K^2\,(v+w) \\ &\quad -\frac{\nu_3}{\lambda_3}\,([\mu_1-\varphi_1\,k_c]\,v-\nu_1\,w)^3 + \cdots,\end{aligned} \tag{49}$$

with

$$\begin{aligned}\alpha_{0i} &= \frac{1}{\lambda_3}\;([\varphi_1\,k_c-\mu_1]\,(\varphi_i\,k_c-\mu_i) - \tilde{\psi}_i\,k_c^2 + \tilde{\varphi}_i\,k_c), && i\geq 2,\\ \alpha_{1i} &= \frac{1}{\lambda_3}\;([\varphi_1\,k_c-\mu_1]\,\varphi_i + \tilde{\varphi}_i - 2\,\tilde{\psi}_i\,k_c), && i\geq 1,\\ \alpha_{2i} &= -\frac{1}{\lambda_3}\;\tilde{\psi}_i, && i\geq 1.\end{aligned}$$

We are now ready for the centre manifold reduction. The transcritical bifurcation without parameters takes place on a two-dimensional invariant manifold that is tangent to the plane spanned by the two eigenvectors associated with the zero eigenvalues. Hence, in our new coordinate system, the centre manifold is tangent to the (K,v)-plane. Therefore, at least locally near the origin, we can express this manifold as the graph of a function $w=H(K,v)$, where $H(0,0)=0$. Since the centre manifold is invariant under the flow of the vector field, we have

$$\dot{w} = \frac{\partial H}{\partial K}\,\dot{K} + \frac{\partial H}{\partial v}\,\dot{v}. \tag{50}$$

Using this invariance condition, together with Eq. (49) for $\dot{w}$, and Eqs. (47) and (48) for $\dot{K}$ and $\dot{v}$, respectively, we can determine the leading coefficients in the polynomial expansion for H and thus eliminate w in the leading terms for the K- and v-equations. Let us consider the expansion for $H(K,v)$ up to order N and write

$$H(K,v) = h_{10}\,K + h_{01}\,v + h_{20}\,K^2 + h_{11}\,K\,v + h_{02}\,u^2 + \cdots.$$

The expression for $\dot{w}$ then starts with

$$\dot{w} = \lambda_3\,w = \lambda_3\,H(K,v) = \lambda_3\,h_{10}\,K + \lambda_3\,h_{01}\,v + \cdots.$$

After some algebraic manipulation it becomes clear that the right-hand-side of Eq. (50) does not contain any linear terms, so we must have $h_{10}=h_{01}=0$. Upon further inspection, one notices that, if $H(K,v)$ contains no linear term in K, then the term $\lambda_3\,h_{20}\,K^2$ on the left-hand-side of Eq. (50) cannot be canceled, because the corresponding term on the right-hand-side has coefficient zero. Note that this does not hold for terms of the form v^2 or $K\,v$. Continuing this argument, there

can be no terms of the form K^i, $0 \leq i \leq N$ in the expansion for $H(K, v)$ up to order N. In other words,

$$H(K, v) = v\,\widehat{H}(K, v)$$

and the dynamics on the centre manifold can be written as Eq. (31), namely

$$\left\{\begin{array}{rcccccl} \dot{K} & = & & & \hat{a}\,v^2 & + & v\,g_1(K, v), \\ \dot{v} & = & \hat{b}\,K\,v & + & \hat{c}\,v^2 & + & v\,g_2(K, v). \end{array}\right.$$

Furthermore, this also means that the coefficients $\hat{a}$, $\hat{b}$ and $\hat{c}$ can simply be read from Eqs. (47) and (48), namely

$$\begin{aligned} \hat{a} &= -\varphi_1 + (\varphi_1^2\,k_c - \tilde{\varphi}_1)\,(\mu_1 - \varphi_1\,k_c), \\ \hat{b} &= \beta_{11}, \\ \hat{c} &= \beta_{02} + \frac{\nu_2}{\lambda_3}\,(\mu_1 - \varphi_1\,k_c)^2. \end{aligned}$$

Using the definitions for $\tilde{\varphi}_1$, β_{11} and β_{02} and after some manipulation using Eq. (29), this leads to the coefficients given in Eq. (32) in Sec. 3.1.